Genet Program Evolvable Mach (2016) 17:409–449
DOI 10.1007/s10710-016-9265-9

# Prediction of expected performance for a genetic programming classifier

**Yuliana Martínez[1] · Leonardo Trujillo[1] · Pierrick Legrand[2] · Edgar Galván-López[3]**

Received: 29 September 2015 / Revised: 7 February 2016 / Published online: 22 February 2016

**Abstract** The estimation of problem difficulty is an open issue in genetic programming (GP). The goal of this work is to generate models that predict the expected performance of a GP-based classifier when it is applied to an unseen task. Classification problems are described using domain-specific features, some of which are proposed in this work, and these features are given as input to the predictive models. These models are referred to as predictors of expected performance. We extend this approach by using an ensemble of specialized predictors (SPEP), dividing classification problems into groups and choosing the corresponding SPEP. The proposed predictors are trained using 2D synthetic classification problems with balanced datasets. The models are then used to predict the performance of the GP classifier on unseen real-world datasets that are multidimensional and imbalanced. This work is the first to provide a performance prediction of a GP system on test data, while previous works focused on predicting training performance. Accurate predictive models are generated by posing a symbolic regression task and solving it with GP. These results are achieved by using highly descriptive features and including a dimensionality reduction stage that simplifies the learning and testing

✉ Leonardo Trujillo
leonardo.trujillo@tectijuana.edu.mx

Yuliana Martínez
ysaraimr@gmail.com

Pierrick Legrand
pierrick.legrand@u-bordeaux.fr

Edgar Galván-López
edgar.galvan@scss.tcd.ie

[1] Tree-Lab, Posgrado en Ciencias de la Ingeniería, Departamento de Ingeniería Eléctrica y Electrónica, Instituto Tecnológico de Tijuana, Tijuana, BC, Mexico

[2] CQFD Team, INRIA Bordeaux, IMB, Université of Bordeaux, Talence, France

[3] School of Computer Science and Statistics, Trinity College Dublin, Dublin, Ireland

process. The proposed approach could be extended to other classification algorithms and used as the basis of an expert system for algorithm selection.

**Keywords** Problem difficulty · Prediction of expected performance · Genetic programming · Supervised learning

## 1 Introduction

Within the field of evolutionary computation (EC) [6] it is not yet clear if a particular algorithm will perform well on a specific problem instance. The “No Free Lunch” (NFL) theorem [70] has provided valuable theoretical and conceptual insights, broadly stating that all search algorithms on average are equivalent when they are evaluated over all possible problems. On the other hand, the NFL theorem does not apply to many common domains of genetic programming (GP) [43], a promising theoretical insight that drives research to develop the best possible GP-based search. Nevertheless, it is by now evident that most GP-based systems tend to perform well on some problem instances while failing on others, with little understanding as to why or when either of those two scenarios will arise [14, 15, 34, 57, 59].

The above issue can be described as the study of problem difficulty, which has been studied in different ways in EC and GP literature. Some methods focus on analyzing the properties of a problem’s fitness landscape [27]. This can be done, for instance, by defining specific classes of functions [20], or by extracting high-level features [14, 15, 34, 57, 59] or statistical properties [4, 8, 9, 13, 26, 47, 62, 69] of the fitness landscape. In the case of standard tree-based GP, where search operators are applied in syntax space, the concept of a fitness landscape is difficult to define given that there is no clear way of determining a general concept of neighborhood for GP representations that are usually highly redundant, which limits the usefulness of such approaches. While some methods have been successfully applied to GP, these are mostly sampling-based techniques that attempt to infer specific types of structures within the underlying fitness landscape, such as: neutrality [8, 11, 12, 42, 72], locality [9, 10], ruggedness [62], deception [56], fitness distance correlation (FDC) [4, 56], fitness clouds [64] and negative slope coefficient (NSC) [66, 67]. In this work, we refer to such methods as evolvability indicators (EIs), which are extensively reviewed in [33] and discussed in the following section.

One notable shortcoming of EIs is that they require an extensive sampling of the search space in order to compute them [2, 46, 65, 68]. This is an important limitation: if we need to know when a particular problem is easy or difficult for an algorithm to solve it may just be easier to run the algorithm and observe its behavior and outcome. Therefore, some researchers have proposed predictive models that take the problem data (or a description of the data) as input, and produce as output a prediction of expected performance, we will refer to such methods as predictors of expected performance (PEPs). Currently, the development of PEPs represents the minority of research devoted to problem difficulty in GP, with only a few recent works. In particular, Graff and Poli [14–18] have studied the development of such predictive models, for symbolic regression, Boolean and time-series problems. While their original work mostly focused on synthetic benchmarks [15], more recent contributions extended their approach to performance prediction in real-world problems [14, 18]. However, in their approach it is necessary to have an extensive knowledge of the real-world problems in advance. Furthermore, their models are intended to predict the performance of the best solution found by GP on the training set of data, they did not address the prediction of performance on unseen test cases.

This paper is an extension of our previous work [57, 59, 60] where PEPs were first proposed for a GP classifier, making several methodological and experimental contributions. First, the PEP models are produced using only simple 2D synthetic datasets that are randomly generated. Second, the PEP models are used to predict the performance of the GP classifier on the test set of data, while previous works mostly focused on predicting performance on the training or learning set [14–18]. Third, accurate predictions are obtained on unseen real-world problems that are multidimensional and contain imbalanced data. On the other hand, previous works [14–18, 57, 59, 60] used the same type of problems (either synthetic or real) for both training and testing. Fourth, to increase PEP accuracy this paper presents an ensemble approach using specialized PEP models called SPEPs. Each SPEP is trained to predict performance within a specific range of classification error. To do so, we use a two-tier approach, where each problem is first classified into a specific group, and then prediction is obtained from the corresponding SPEP which was trained for that group of problems. Finally, it is reasonable to state that the proposed approach could be applied to predict the performance of GP on other learning problems.

The remainder of this paper proceeds as follows. Section 2 reviews related work and Sect. 3 provides a short survey of GP-based classification. The basic PEP strategy is outlined and evaluated in Sect. 4. Afterwards, Sect. 5 introduces the proposed ensemble strategy based on SPEPs and provides experimental results. Finally, Sect. 7 contains conclusions and future work.

## 2 Related work

Determining problem difficulty has been an important issue in EC for several years [35]. From an algorithmic perspective, problem difficulty can be related to the total runtime (or memory) required to find an optimal solution. Recently, He et al. [20] took this view one step further, to analytically define broad classes of fitness functions which allowed them to demonstrate that easy functions define unimodal fitness landscapes, while hard functions define deceptive landscapes for a $(1 + 1)$ ES. However, it is important to remember that the difficulty of a particular problem depends upon the solution method. Therefore, in what follows we will try to limit our overview to GP-related research.

### 2.1 Evolvability indicators

The fitness landscape has dominated the way geneticists think about biological evolution and has been adopted by the EC community as a way to visualize evolution dynamics [71]. Formally, a fitness landscape can be defined as a triplet $(x, \chi, f)$, where $x$ is a set of configurations, $\chi$ is a notion of neighborhood, distance or accessibility on $x$, and $f$ is a fitness function [54]. The local and global structure of the fitness landscape describes the underlying difficulty of a search. However, in the case of standard GP [30] the concept of a fitness landscape is not clearly defined [27]. To overcome this, some works have constructed synthetic problems; such as the Royal Tree problem [44] or the K-landscapes model [62], where the goal of the search is defined as a particular tree structure with a specific syntax. Unfortunately, such models are not realistic since the space of possible programs is highly redundant [30] in most domains, and the goal is not a particular syntax but a particular expected output, also known as semantics [36, 63]. Therefore, some researchers have proposed variants of GP that explicitly account for program semantics. In semantic space the fitness landscape is clearly defined and unimodal. This has lead researchers to develop specialized search operators that modify program syntax while geometrically bounding the semantics of the generated offspring, this is known as geometric semantic GP (GSGP) [38]. Nevertheless, such approaches are still problematic since the size of the evolved programs grows exponentially with every generation, a limitation that is not easily solved [50]. This work will focus on measures of problem difficulty for standard GP systems [29], but could be applied to other supervised learning systems including GSGP.

In general, most meta-heuristics work under the assumption that the fitness of a candidate solution, a point on the fitness landscape, is positively correlated with the fitness of its (some) neighbors. Such a property can be defined as the *evolvability* of a landscape [1, 41]. EIs extract a numerical indicator of a specific property of the fitness landscape to provide a measure of the evolvability within the landscape. Malan et al. [33] presents a comprehensive survey of EIs and other forms of fitness landscape analysis.

Those that have been studied in GP literature include neutrality [8, 26], locality [9, 47], ruggedness [25, 62], fitness distance correlation (FDC) [4, 24, 56], fitness clouds [69] and the negative slope coefficient (NSC) [64]. While these approaches can sometimes provide good estimates of problem difficult for GP, they suffer from two practical limitations. First, for each new problem instance they require a large amount of data, by sampling the search space or performing several runs. Second, they cannot estimate the actual quality of the solution found, which can be important if we want to choose the best algorithm to use for a new problem, and if such a choice must be made in real-time. Indeed, Malan et al. [33] point out that a possible way forward is to build a mapping that can estimate algorithm performance based on a set of descriptive features of the problem, an approach that would provide a more practical measure of problem difficulty and allow us to choose the best algorithm for the specific task. Malan and Engelbrecht [32] attempted to find a link between EIs and algorithm performance for particle swarm optimization.

## 2.2 Performance prediction

PEPs predict the performance of a GP search on an unseen problem instance without performing the search or sampling the solution space. These models have been derived using a machine learning approach [14, 15, 34, 57, 59]. The performance of GP on a set of problems and a description of those problems are used to pose a supervised learning task. A promising feature of PEPs is that they are not only useful for GP, they can also be used to predict the performance of other algorithms [16, 59].

Graff and Poli [16] proposed linear predictive models based on a sampling of the fitness landscape, given by

$$P(\mathbf{t}) \approx a_0 + \sum_{\mathbf{s}\in\mathcal{S}} a_{\mathbf{s}} \cdot d(\mathbf{s},\mathbf{t}), \tag{1}$$

where $P(\mathbf{t})$ is the predicted performance, $\mathbf{t}$ is the target functionality, $d(\mathbf{s},\mathbf{t})$ is a distance measure,[1] $\mathcal{S}$ is the set of all possible program outputs, also known as semantic space [38], and where each $\mathbf{s}$ represents the vector of program outputs obtained from the set of fitness cases used to define a particular problem, also known as the semantics of the program [36]. In other words, Graff and Poli [16] derive PEPs by sampling semantic space $\mathcal{S}$. These models were tested on symbolic regression and 4-input Boolean problems with promising results.

The second and more recent approach towards building a PEP focuses on the problem data [14, 17, 18, 34, 57–60] and proceeds as follows. Assume we want to solve a supervised learning problem $p$ with a GP search, where fitness is given by a cost function that must be minimized, such as an error measure. Let us define the performance of the GP algorithm as the associated error of the best solution found during training when it is evaluated on a particular set of fitness cases $T$, call this quantity $F_T(p)$. The goal is to predict $F_T(p)$, so first we construct a feature vector $\beta = (\beta_1, \beta_2, \ldots, \beta_N)$ of $N$ distinct features that describe the main properties of $p$. Then, a PEP is function $K$ such that

$$F_T(p) \approx K(\beta). \tag{2}$$

Notice that the form of $K$ is not a priori restricted in any way. Graff and Poli [17] use a linear function similar to the one used in their previous work [16]. Using this approach the feature vector $\beta$ should be designed specifically for the domain of $p$. For example, features designed for symbolic regression and Boolean problems are proposed in [17], and the results show that the predictive accuracy surpasses that of the fitness-based models proposed in [16]. However, their work did not scale well to real-world cases. For instance, in [14, 18] the authors built PEPs to predict performance on real-world problems, but require information obtained from runs performed on similar problem instances, models built with simpler synthetic problems could not be used. It was not trivial to map multidimensional problems to the proposed feature space since the training problems were much simpler with a small number of dimensions. It would be impractical to consider all possible dimensionalities during training. This is an important limitation in building PEPs, since it is not trivial to have all the possible versions of the same problem. Moreover, in the proposals made by Graff and Poli [14, 17, 18] the models predicted the

[1] Such a distance measure is a common fitness function for many application domains of GP, particularly for symbolic regression problems.

performance of the GP system on the training set of fitness cases; i.e., $T$ was the training set. While certainly of importance, performance on the training set may not be useful if the algorithm overfits the training examples, which happens often in real-world scenarios.

In previous work [57, 59, 60], we used a similar approach to predict the performance of a GP-classifier using descriptive features that characterize the geometry of the data distribution in feature space. The PEPs where built using quadratic linear models and non-linear GP models, the latter achieving the best performance on synthetic problems. However, it was not clear how well the PEPs generalized to unseen problem instances, particularly to real-world problems with imbalanced datasets and larger feature spaces than those used to train the models, a similar difficulty pointed out in [14, 18]. The current work extends our previous contributions by performing the learning process on 2D synthetic problems and testing on a wide variety of real-world datasets. Moreover, an important contribution of this work is that the PEP models are used to predict the performance of the best solution found by GP when it is evaluated on the test set of data. To achieve improved performance this work also proposes a two-tiered ensemble approach using specialized PEP models and a preprocessing stage for dimensionality reduction.

## 3 Classification with GP

In machine learning one of the most common tasks is supervised classification [28]. The general task can be stated as follows. Given a pattern $\mathbf{x} \in \mathbb{R}^P$ assign the correct class label among $C$ distinct classes $\omega_1, \ldots, \omega_C$, using a training set $\mathcal{T}$ of P-dimensional patterns with a known label. The idea is to build a mapping $g(\mathbf{x}) : \mathbb{R}^P \rightarrow C$, that assigns each pattern $\mathbf{x}$ to a corresponding class $\omega_i$, where $g$ is derived based on the evidence provided by $\mathcal{T}$. GP has been widely used to address this problem [40, 53, 57, 73–75]. In general, GP can be applied to classification following three general approaches:

1. Feature selection and construction [39, 40, 48, 57, 75].
2. Model extraction [3, 55, 61, 73, 74].
3. Learning ensemble classifiers [21, 23, 30].

Feature selection and construction is also known as preprocessing of the problem data. These approaches use GP to either select the most interesting problem features or to construct new features that simplify the classification problem. These techniques are often described as either filter [19, 39, 57, 75] or wrapper approaches [40, 48, 51]. In the former, feature construction is done independently of the model used to build the classifier, while in the latter fitness assignment is based on the performance of a classifier. On the other hand, model extraction with GP is used to build specific types of classifiers, such as decision trees [55, 61], classification rules [3, 45] and discriminant functions [74]. Finally, ensemble classifiers are used to improve the quality of the classification task by using not only a single classifier, but a group of them, each one providing a different output [21, 23, 30].

### 3.1 Probabilistic genetic programming classifier

In this work we derive PEPs for the probabilistic genetic programming classifier (PGPC) proposed in [75], a feature construction method. PGPC was chosen due to its simplicity and strong performance on real-world problems [53]; while other GP-based classifiers could have been used this is left as future work. In PGPC, GP is used to evolve a mapping $g(\mathbf{x}) : \mathbb{R}^P \rightarrow \mathbb{R}$ that transforms each input pattern $\mathbf{x}$ into a point on the real line. Furthermore, it is assumed that the behavior of $g$ can be modeled using multiple Gaussian distributions, each corresponding to a single class [75]. The distribution of each class $\mathcal{N}(\mu, \sigma)$ is derived from the examples provided for it in set $\mathcal{T}$ , by computing the mean $\mu$ and standard deviation $\sigma$ of the outputs obtained from $g$ on these patterns. Then, from the distribution $\mathcal{N}$ of each class a fitness measure can be derived using Fisher's linear discriminant; for a two class problem it proceeds as follows. After the Gaussian distribution $\mathcal{N}$ for each class are derived, a distance is required. In [75], Zhang and Smart propose a distance measure between both classes as

$$d = 2 * \frac{|\mu_1 - \mu_2|}{\sigma_1 + \sigma_2}, \tag{3}$$

where $\mu_1$ and $\mu_2$ are the means of the Gaussian distribution of each class, and $\sigma_1$ and $\sigma_2$ their standard deviations. When this measure tends to 0, it is the worst case scenario because the mappings of both classes overlap completely, and when it tends to $\infty$, it represents the optimal case with maximum separation. To normalize the above measure, the fitness for an individual mapping $g$ is given by

$$f_d = \frac{1}{1 + d}. \tag{4}$$

After executing PGPC, the best individual found determines the parameters for the Gaussian distribution $\mathcal{N}_i$ associated to each class. Then, a new test pattern $\mathbf{x}$ is assigned to class $i$ when $\mathcal{N}_i$ gives the maximum probability; performance is measured by the total classification error (CE) on test data.

## 4 PEP: predictor of expected performance

The general goal of this work is to build models that can predict the performance of a GP-classifier (PGPC) without executing the search or sampling the problem's search space. The general proposal is depicted in Fig. 1, where for a given classification problem we do the following. First, apply a preprocessing step to simplify the feature extraction process and deal with multidimensional representations. Second, perform feature extraction to obtain an abstraction of the problem.

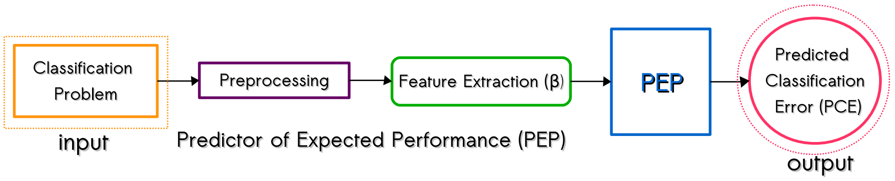
Classification Problem
input
Preprocessing
Feature Extraction (β)
Predictor of Expected Performance (PEP)
PEP
Predicted Classification Error (PCE)
output

**Fig. 1** Block diagram of the proposed PEP approach. Given a classification problem, the goal is to predict the performance of a GP classifier on the test data, in this case PGPC

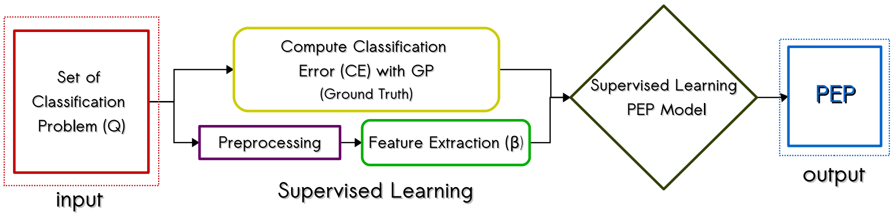
Set of Classification Problem (Q)
input
Compute Classification Error (CE) with GP (Ground Truth)
Preprocessing
Feature Extraction (β)
Supervised Learning
Supervised Learning PEP Model
PEP
output

**Fig. 2** The methodology used to build the PEP model. Given a set $\mathcal{Q}$ of synthetic classification problems: (1) compute the CE$\mu$ of PGPC on all problems; (2) apply a preprocessing for dimensionality reduction; (3) extract the feature vector $\beta$ from the problem data; and (4) learn the predictive model using GP

Third, use a PEP model that takes as input the extracted features and produces as output the predicted classification error (PCE) on the testing set.

Moreover, to derive the PEP models we use a supervised learning methodology, depicted in Fig. 2. This process takes as input a set of synthetic classification problems $\mathcal{Q}$ and produces as output the PEP model as follows:

1. Compute the average classification error (CE$\mu$) on the test data by PGPC for each $p \in \mathcal{Q}$.
2. Apply a preprocessing for dimensionality reduction using principal component analysis (PCA), and take the first $m$ principal components to represent the problem data.
3. Perform feature extraction on the transformed data using statistical and complexity measures to build a feature vector $\beta$ for each $p \in \mathcal{Q}$.
4. Finally, using the set of feature vector/performance pairs $\{(\beta_i, \text{CE}\mu_i)\}$ formulate a supervised symbolic regression problem and solve it using GP.

### 4.1 Synthetic classification problems

A set of synthetic classification problems was generated to learn our PEP models. Specifically, 500 binary classification problems were generated using Gaussian mixture models (GMMs) with either unimodal or multimodal classes, with different amounts of class overlap. All class samples lie within the closed 2-D interval $x, y \in [-10, 10]$, and 200 sample points were randomly generated for each class.

The parameters for the GMM of each class were randomly chosen using a uniform distribution in the following ranges:

1. Number of Gaussian components: $\{1, 2, 3\}$.
2. Median of each Gaussian component for each dimension: $[-3, 3]$.
3. Each element of the covariant matrix of each Gaussian component: (0, 2].
4. The rotation angle of each covariance matrix: $[0, 2\pi]$.
5. Proportion of samples generated with each Gaussian component: [0, 1].

## 4.2 PGPC classification error

For each problem $p \in \mathcal{Q}$ we perform 30 runs of PGPC, randomly choosing the training and testing sets in each run. Then, the mean classification error CE$\mu$ is computed by the average of the test performance achieved by the best solutions found in each run. The parameters of the PGPC system are given in Table 1, a tree-based GP algorithm with dynamic depth bloat control [50], implemented using Matlab and the GPLAB toolbox [49]. Figure 3 presents some examples, showing the problem data, the CE$\mu$ achieved by PGPC and the standard deviation $\sigma$ over all runs. The problems are ordered from the lowest CE$\mu$ (easiest problem, depict in Fig. 3a) to the highest, CE$\mu$ (hardest problem, depict in Fig. 3f).

Figure 4 summarizes PGPC performance over all 500 synthetic problems in $\mathcal{Q}$. Figure 4a plots the CE$\mu$ for each problem, ordered from the lowest to the highest error. On the other hand, Fig. 4b shows an histogram of PGPC performance,

**Table 1** Parameters for the PGPC algorithm

| Parameter | Description |
|---|---|
| Population size | 200 Individuals |
| Generations | 200 Generations |
| Initialization | *Ramped half-and-half*, with six levels of maximum depth |
| Operator probabilities | Crossover $p_c = 0.8$; mutation $p_\mu = 0.2$ |
| Function set | $\left\{+, -, *, /, \sqrt{\cdot}, sin, cos, log, x^y, \vert \cdot \vert, if\right\}$ |
| Terminal set | $\{x_1, \ldots, x_i, \ldots, x_P\}$ where each $x_i$ is a dimension of the data patterns $\mathbf{x} \in \mathbb{R}^P$ |
| Bloat control | Dynamic depth control |
| Initial dynamic depth | 6 Levels |
| Hard maximum depth | 20 Levels |
| Selection | Tournament, size 3 |
| Survival | Keep best elitism |
| Training data | 70 % |
| Testing data | 30 % |
| Runs | 30 |

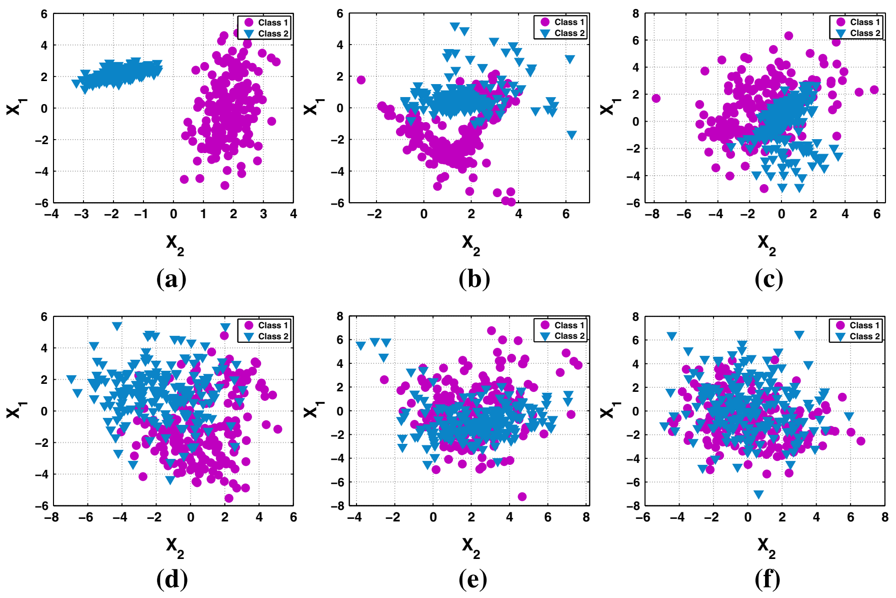

**Fig. 3** The scatter plots show examples of synthetic classification problems, specifying the CE$\mu$ and standard deviation $\sigma$ achieved by PGPC. These ordered from the lowest CE$\mu$ (easiest depict in Fig. 3a) to the highest CE$\mu$ (hardest depict in Fig. 3f). **a** CE$\mu = 0\, \sigma = 0$. **b** CE$\mu = 0.14\, \sigma = 0.03$. **c** CE$\mu = 0.17\, \sigma = 0.03$. **d** CE$\mu = 0.21\, \sigma = 0.03$. **e** CE$\mu = 0.36\, \sigma = 0.04$. **f** CE$\mu = 0.46\, \sigma = 0.04$

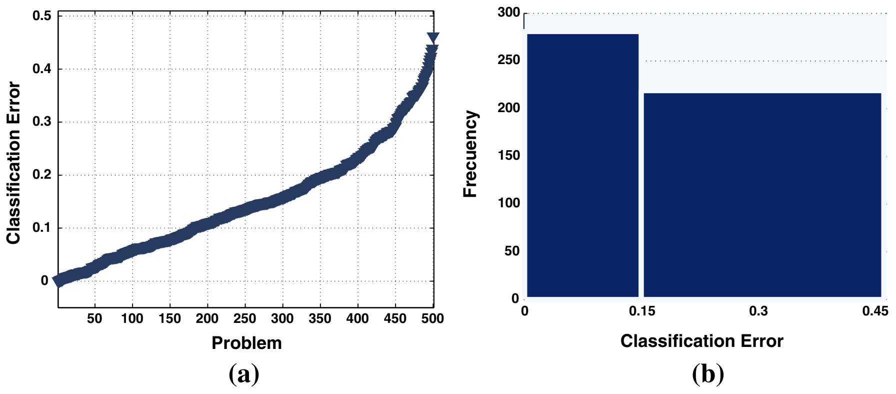

**Fig. 4** Performance of PGPC over all 500 synthetic problems in $\mathcal{Q}$; where **a** shows the CE$\mu$ for each problem, ordered from the easiest to the hardest; and **b** shows the histogram over CE$\mu$

quantifying how many problems are solved with a particular CE$\mu$. We arbitrarily set a threshold such that problems in the range $0 \leq$ CE$\mu \leq 0.15$ are considered “easy” and the rest are considered to be “hard”. From this perspective the plot reveals that randomly generated problems produce a biased distribution, where most problems are easy to solve. Since we intend to use this set to pose a supervised learning task, this would induce an unwanted bias. Therefore, we subsample $\mathcal{Q}$ to get a more

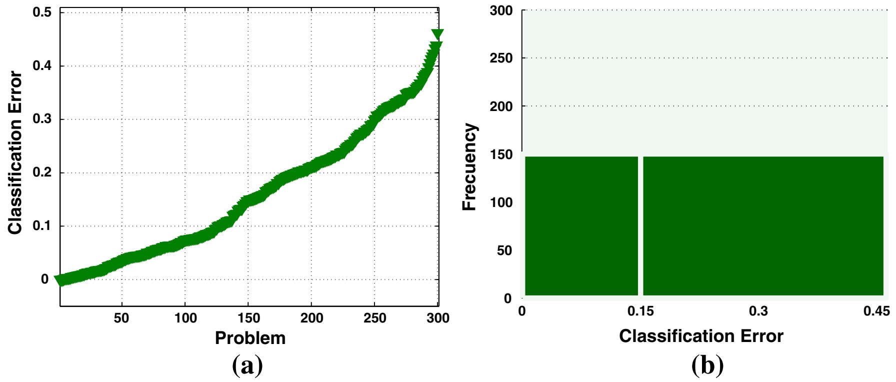

**Fig. 5** Performance of PGPC over all 300 synthetic problems in $\mathcal{Q}' \subset \mathcal{Q}$; where **a** shows the CE$\mu$ for each problem, ordered from the easiest to the hardest; and **b** shows the histogram over CE$\mu$

balanced distribution over CE$\mu$. The new set consists of 300 problems, and Fig. 5 summarizes PGPC performance over this new set $\mathcal{Q}'$. Notice that the performance plot for $\mathcal{Q}' \subset \mathcal{Q}$ is similar to the one obtained for $\mathcal{Q}$ (see Fig. 5a), but now the distribution over CE$\mu$ is flat (Fig. 5b), providing a more balanced learning set.

### 4.3 Preprocessing

Previous work has found that PEP models can predict GP performance accurately for small scale synthetic problems [15–17, 34, 57–60], but accuracy degrades for real-world problems with high dimensional data [14, 18]. This is due to the fact that feature extraction (the next step in the PEP approach) fails at extracting meaningful information in high dimensional spaces [14, 18]. To deal with this issue, we apply a dimensionality reduction preprocessing of the problem data using PCA [5]. We propose to take the first $m$ principal components to represent the data of each problem. In particular, we set $m = 2$ in all experiments reported here. In this way, all problems are reduced to the same number of dimensions used in the synthetic training set.

### 4.4 Feature extraction

The goal of this step is to extract a set of descriptive measures from each problem. In this work, we use a subset of the features proposed in [52] and [22]. Those works attempted to develop meta-representations of classification problems. A wider set of features was previously tested in [57–60], but the present work only uses those features that showed the highest correlation with CE$\mu$. We also propose three new descriptors based on the Canberra distance; each measure is presented next.

*Geometric mean (SD)* measures the homogeneity of covariances [37, 52]. This quantity is related to a test of the hypothesis that all populations have a common covariance structure; i.e.. to the hypothesis $H_0 : \sum_1 = \sum_2$, which can be tested via Box's $M$ test statistic (MTS), that can be re-expressed as

$$SD = exp\left\{\frac{MTS}{m\sum_{i=1}^{C}(n_i - 1)}\right\} \tag{5}$$

where $C$ is the number of classes, $n_i$ is the number of the instances for $i$th class and $m$ is the number of dimensions. The SD is strictly greater than unity if the covariances differ, and is equal to unity if and only if the MTS is zero.

*Feature efficiency (FE)* measures the amount by which each feature dimension contributes to the separation of both classes. This measure is computed for the $i$th dimension by

$$FE_i = \left(1 - \frac{\eta_i}{tp}\right) \tag{6}$$

where $\eta_i$ represent the number of points inside the overlapping region and $tp$ is the total number of sample points; as seen in Fig. 6a. Finally, we define $FE = max(\{FE_i\})$ with $i = [1, m]$ for any given problem with $m$ dimensions.

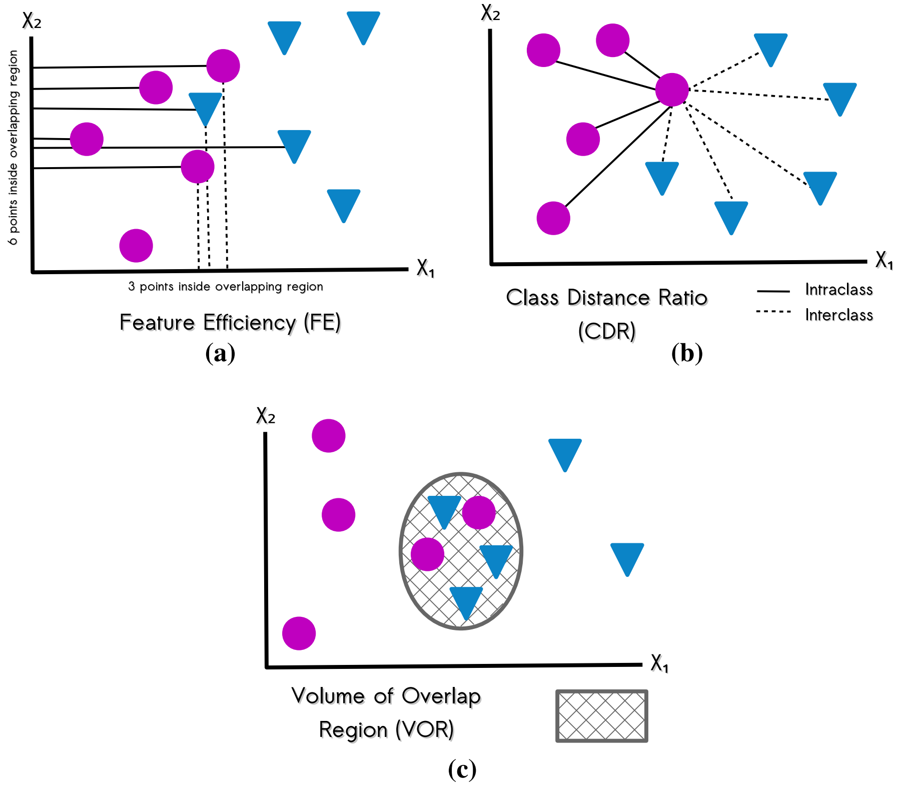
X2
6 points inside overlapping region
X1
3 points inside overlapping region
Feature Efficiency (FE)
(a)
X2
X1
Class Distance Ratio (CDR)
Intraclass
Interclass
(b)
X2
X1
Volume of Overlap Region (VOR)
(c)

**Fig. 6** These figures depict the complexity features used to describe each classification problem as suggested in [22], where **a** feature efficiency (FE); **b** class distance ratio (CDR); and **c** volume of overlap region (VOR)

*Class distance ratio (CDR)* compares the dispersion within the classes to the gap between the classes [22]. For each data sample, compute the Euclidean distance to its nearest neighbor within the class (intraclass distance) and nearest-neighbor from the other class (interclass distance), as shown in Fig. 6b. The CDR is the ratio of the averages of all intraclass and interclass distances.

*Volume of overlap region (VOR)* provides an estimate of the amount of overlap between both classes in feature dimension space [22]. The VOR is computed by finding, for each dimension, the maximum and minimum value of each class and then calculating the length of the overlap region. The length obtained from each dimension is then multiplied to measure the overlapping region, as depicted in Fig. 6c. The VOR is zero when there is at least one dimension in which the two classes do not overlap.

*Canberra distance (CD)* provides a numerical measure of the distance between pairs of points in a vector space. Suppose a problem has $m$ feature dimensions, we take a rank statistic of the samples of each class, call it $x_i$ for class 1 and $y_i$ for class 2, for the $i$th dimension. This produces two vectors $\mathbf{x}$ and $\mathbf{y}$, such that $\mathbf{x} = (x_1, \ldots, x_m)$ and $\mathbf{y} = (y_1, \ldots, y_m)$. The CD is given by

$$CD(\mathbf{x}, \mathbf{y}) = \frac{1}{m} \sum_{i=1}^{m} \frac{|x_i - y_i|}{|x_i| + |y_i|}. \tag{7}$$

In this work, we use the CD to describe the distance between both classes using three rank statistics: (1) CD-1 uses the 1st quartile; (2) CD-2 uses the median; and (3) CD-3 uses the 3rd quartile.

The set of descriptive measures discussed above helps to minimize the information about each problem. Now, analyzing the algorithmic complexity (big O notation) of the measures, these do not represent a significant computational cost. For instance, the FE, VOR, CD-1, CD-2 and CD-3 features mainly depend on a sorting process, which can have a complexity of $O(n \, log n)$ where $n$ is the number of instances of the problem. Moreover, the SD relies on computing the covariance matrix of the data which has a complexity of $O(n^2)$. Similarly, to compute the CDR feature we need to do all pairwise comparisons, which also has a complexity of $O(n^2)$.

Figure 7 provides a visual description of the descriptive power of each feature. The figure shows scatter plots where each point corresponds to a single problem $p \in \mathcal{Q}'$, the x-axis is a particular feature (SD, FE, CDR, VOR, CD-1, CD-2 and CD-3) and the y-axis is the associated CE$\mu$. The caption of Fig. 7 also gives the Pearson's correlation coefficient $\rho$. It is evident that all of the chosen features are correlated with PGPC performance, in particular FE, VOR, CDR, CD-1 and CD-3 show the highest correlation.

## 4.5 Supervised learning of PEP models

It is now possible to pose a symbolic regression problem using the set $T = \{(\beta_i, \text{CE}\mu_i)\}$ with $i = 1, \ldots, |\mathcal{Q}'|$, where the goal is to evolve a model $K$ that can predict each CE$\mu_i$ using $\beta_i$ as input. Previous works have used several types of

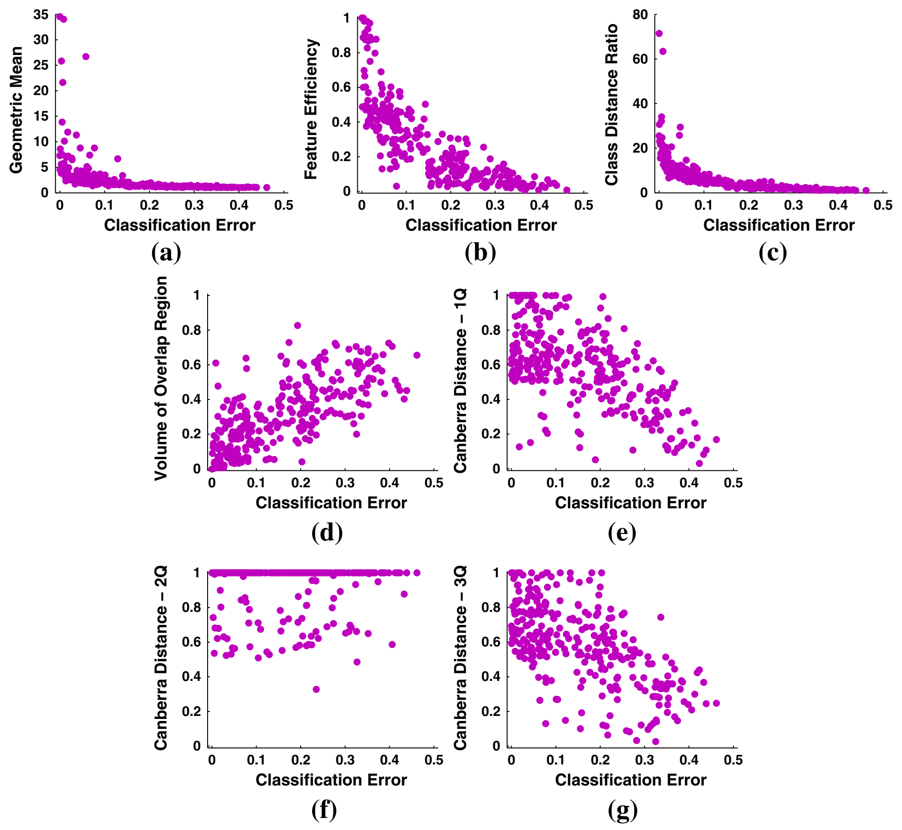

**Fig. 7** Scatter plots show the relationship between the CE$\mu$ (x-axis) and each descriptive feature (y-axis) for all problems $p \in \mathcal{Q}'$, where $\rho$ specifies Pearson's correlation coefficient. **a** SD: $\rho = -0.42$, **b** FE: $\rho = -0.78$, **c** CDR: $\rho = -0.62$, **d** VOR: $\rho = -0.72$, **e** CD-1: $\rho = -0.62$, **f** CD-2: $\rho = -0.03$ and **g** CD-3: $\rho = -0.61$

linear models [17, 34, 57–60], but [57, 59, 60] showed that non-linear models evolved with GP achieved higher prediction accuracy.

Therefore, in this work we use a tree-based GP, configured with the parameters given in Table 2. Three versions of the problem are posed, each with a different terminal set defined as subsets of all extracted features (4F, 5F, 7F) as specified in Table 3. Set 4F uses the features with the four highest correlation coefficients (FE, CDR, VOR and CD-1), set 5F uses the features with the five highest correlation coefficients (SD, FE, CDR, VOR and CD-1), and 7F uses all of the seven features. The function set is defined as $F = \left\{+, -, *, /, \sqrt{}, sin, cos, log, x^y, |\cdot|, if\right\}$. Finally the fitness function is computed by the root mean squared error (RMSE) between the predicted CE and the true CE$\mu_i$, given by

$$f(K) = \sqrt{\frac{\sum_{i=1}^{n}(K(\beta_i) - CE\mu_i)^2}{n}}. \tag{8}$$

**Table 2** Parameters for the GP used to derive PEP models for PGPC algorithm

| Parameter | Description |
|---|---|
| Population size | 200 Individuals |
| Generations | 100 Generations |
| Initialization | *Ramped half-and-half*, with 6 levels of maximum depth |
| Operator probabilities | Crossover $p_c = 0.8$; mutation $p_\mu = 0.2$ |
| Hard maximum depth | 12 Levels |
| Selection | Tournament, size 3 |
| Survival | Keep best elitism |
| Runs | 100 |

**Table 3** Three different features sets used as terminal elements for the symbolic regression GP algorithm

| Feature vector $\beta$ | |
|---|---|
| *4F* | FE, CDR, VOR and CD-1 |
| *5F* | SD, FE, CDR, VOR and CD-1 |
| *7F* | SD, FE, CDR, VOR, CD-1, CD-2 and CD-3 |

## 4.6 Testing the PEP models

For each version of the symbolic regression problem defined above (with different feature sets), we performed 100 runs using two different test scenarios: (1) train and test the PEP models using only synthetic problems; and (2) train with synthetic problems and test with real-world problems. In the first scenario, we use 70 % of the problems for training and the rest for testing, generating a random partition of the set of problems $\mathcal{Q}'$ for each run. This is the simplest scenario, since both the training and testing problems are generated in the same manner. In the second scenario, we test the PEP models trained with synthetic problems and evaluate their predictions on many real-world datasets, a more challenging scenario since the real-world problems have high dimensional data, imbalanced classes and different data distributions.

### *4.6.1 Testing on synthetic classification problems*

Table 4 summarizes the performance of the evolved PEPs, showing the median of the RMSE of the best solution found in each run for the training and testing sets, as well as the RMSE and Pearson's correlation coefficient $\rho$ of the best solution found. The table presents three rows of results, one for each feature set (PEP-4F, PEP-5F and PEP-7F). The numerical results are encouraging, suggesting that the PEP models can accurately predict PGPC performance. Moreover, there is a very small difference between training and testing performance, suggesting that the PEP models are not overfitted.

**Table 4** Prediction performance of the evolved PEPs applied on the synthetic problems using each feature set (4F, 5F and 7F, see Table 3)

| | Median training RMSE | Median testing RMSE | Best RMSE | Best correlation |
|---|---|---|---|---|
| PEP-4F | 0.0320 | 0.0375 | 0.0318 | 0.9634 |
| PEP-5F | **0.0317** | **0.0362** | **0.0295** | **0.9688** |
| PEP-7F | 0.0326 | 0.0364 | 0.0317 | 0.9636 |

Performance is given based on the RMSE and Pearson's correlation coefficient, with bold indicating the best performance

Figure 8 shows plots in three rows, where in each row we plot each feature set (PEP-4F, PEP-5F and PEP-7F). The plots on the left-hand side column show the PCE of the best PEP model and the true CE$\mu$ for all synthetic problems, specifying the RMSE in the caption. The plots on the right-hand side column show the CE$\mu$ and PCE as scatter plots, specifying the Pearson's correlation coefficient $\rho$ in the caption. The evolved PEPs produce accurate predictions with all feature sets.

### *4.6.2 Testing on real-world classification problems*

This section presents the results of testing the best evolved PEPs to predict the testing error of PGPC on real-world problems. To this end, 22 real-world datasets are chosen from the University of California Irvine (UCI) machine learning repository [31], summarized in Table 5. Since our PEPs only consider binary classification, we use these datasets to build 40 binary classification problems. The problems are summarized in Table 6, specifying the name of the dataset and the classes used to define each problem, the number of total samples and the imbalance percentage of each problem computed as $\frac{a-b}{c}$ where $a$ and $b$ are respectively the number of samples in the minority and majority class, and $c$ is the total number of samples. Notice that the synthetic problems used to train the PEPs are completely balanced and relatively small problems in terms of number of samples, while the real-world problems are considerably more varied. In particular, considering class imbalance Fig. 9 shows an histogram of the number of problems with different amounts of imbalance percentage.

Before testing the evolved PEP models, we compute the CE$\mu$ achieved by PGPC using 30 independent runs. PGPC performance is summarized in Fig. 10, showing: (a) the CE$\mu$ for each problem and (b) the histogram over CE$\mu$. Figures 11 presents scatter plots of each descriptive feature (x-axis) and the CE$\mu$ (y-axis) of each problem, specifying the corresponding Pearson's correlation coefficient $\rho$ in the caption. The figures show that the best correlated features with CE$\mu$ are FE and CD-1, respectively with $\rho$ values of $-0.73$ and $-0.71$. The rest of the features do not show particularly good correlation values, with SD clearly being the worst.

These results are different to what was observed on the synthetic problems. While VOR, CDR and CD-3 showed absolute correlation values above 0.6 on synthetic datasets, they were all below 0.44 on the real-world problems. This difference was particularly marked for SD, on synthetic problems the correlation

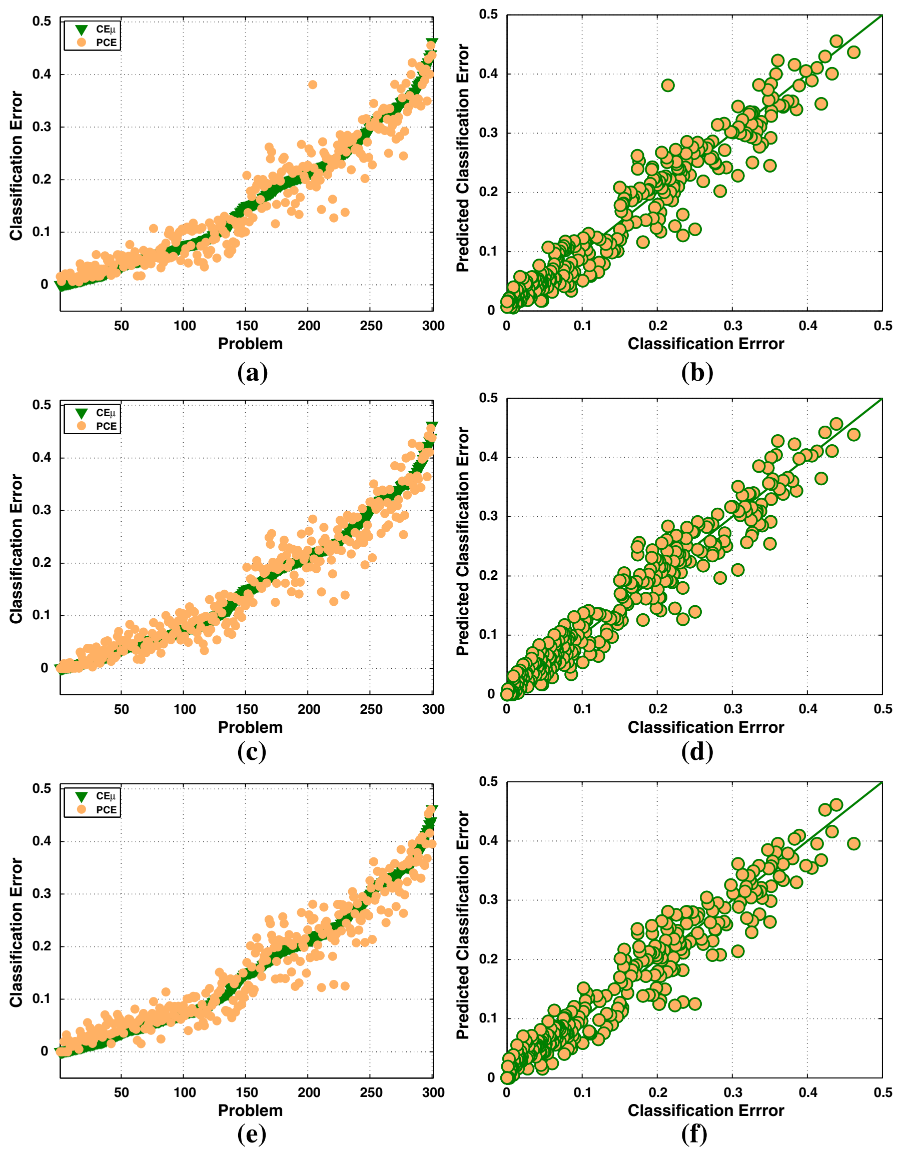

**Fig. 8** Figures show for synthetic problems, the performance prediction of the best PEP models evolved with the different feature set, each row belongs to each feature set: PEP-4F (*top*), PEP-5F (*middle*) and PEP-7F (*bottom*). *Plots on the left-hand side column* show the PCE of the best solution and the known CE$\mu$. The *right-hand side column* show scatter plots of the PCE and the CE$\mu$. **a** *PEP-4F*: RMSE $= 0.0318$, **b** *PEP-4F*: $\rho = 0.9634$, **c** *PEP-5F*: RMSE $= 0.0295$, **d** *PEP-5F*: $\rho = 0.9688$, **e** *PEP-7F*: RMSE $= 0.0317$ and **f** *PEP-7F*: $\rho = 0.9636$

**Table 5** Real-world datasets from the UCI machine learning repository used in this work

| No. | Problem | Classes | Dimensions | Description |
|---|---|---|---|---|
| 1 | Balance scale | 3 | 4 | Balance scale weight and distance database |
| 2 | Breast cancer wisconsin | 2 | 8 | Original Wisconsin Breast Cancer Database |
| 3 | Breast tissue | 6 | 9 | Dataset with electrical impedance measurements of freshly excised tissue samples from the breast |
| 4 | Cardiotocography | 3 | 23 | Fetal cardiotocograms (CTGs) were automatically processed and the respective diagnostic features measured |
| 5 | EEG eye state | 2 | 15 | All data is from one continuous EEG measurement with the Emotiv EEG Neuroheadset |
| 6 | Fertility | 2 | 10 | 100 volunteers provide a semen sample analyzed according to the WHO 2010 criteria |
| 7 | Glass | 6 | 10 | From USA Forensic Science Service; 6 types of glass |
| 8 | Indian liver patient | 2 | 32 | This data set contains 416 liver patient records and 167 non liver patient records |
| 9 | Ionosphere | 2 | 32 | Classification of radar returns from the ionosphere |
| 10 | Iris | 3 | 4 | The data set contains 3 classes of 50 instances each, where each class refers to a type of iris plant |
| 11 | Parkinsons | 2 | 22 | Oxford Parkinson's Disease Detection Dataset |
| 12 | Pima Indians diabetes | 2 | 8 | From National Institute of Diabetes and Digestive and Kidney Diseases |
| 13 | Retinopathy | 2 | 19 | This dataset contains features extracted from the Messidor image set to predict whether an image contains signs of diabetic retinopathy or not |
| 14 | Red wine | 6 | 11 | The goal is to model wine quality based on physicochemical tests |
| 15 | Seed | 3 | 7 | The examined group comprised kernels belonging to three different varieties of wheat |
| 16 | Sonarall | 2 | 60 | The task is to train a network to discriminate between sonar signals bounced off a metal cylinder and those bounced off a roughly cylindrical rock |
| 17 | Tae | 3 | 5 | The data consist of evaluations of teaching performance; scores are "low", "medium", or "high" |
| 18 | Vertebral-column 2C | 2 | 6 | Biomedical data set built by Dr. Henrique da Mota |
| 19 | Vertebral-column 3C | 3 | 6 | Biomedical data set built by Dr. Henrique da Mota |
| 20 | White wine | 6 | 11 | The goal is to model wine quality based on physicochemical tests |
| 21 | Wine | 3 | 13 | Using chemical analysis determine the origin of wines |
| 22 | Zoo | 7 | 3 | Artificial, 7 classes of animals |

**Table 6** The 40 real-world binary classification problems based on the UCI datasets

| No. | Problem | Classes | Instances | Imbalance % |
|---|---|---|---|---|
| 1 | Balance scale | 1–3 | 576 | 0 |
| 2 | Breast cancer wisconsin | 1–2 | 699 | 31 |
| 3 | Breast tissue | 1–2 | 36 | 17 |
| 4 | Breast tissue | 1–3 | 39 | 8 |
| 5 | Breast tissue | 1–4 | 37 | 14 |
| 6 | Breast tissue | 2–3 | 33 | 9 |
| 7 | Breast tissue | 2–4 | 31 | 3 |
| 8 | Breast tissue | 3–4 | 34 | 6 |
| 9 | Cardiotocography | 1–2 | 1950 | 70 |
| 10 | Cardiotocography | 1–3 | 1831 | 81 |
| 11 | Cardiotocography | 2–3 | 471 | 26 |
| 12 | EEG eye state | 1–2 | 8388 | 17 |
| 13 | Fertility | 1–2 | 100 | 76 |
| 14 | Glass | 1–2 | 146 | 4 |
| 15 | Glass | 1–6 | 99 | 41 |
| 16 | Glass | 2–6 | 105 | 45 |
| 17 | Indian liver patient | 1–2 | 579 | 43 |
| 18 | Ionosphere | 1–2 | 351 | 28 |
| 19 | Iris | 1–2 | 100 | 0 |
| 20 | Iris | 1–3 | 100 | 0 |
| 21 | Iris | 2–3 | 100 | 0 |
| 22 | Parkinsons | 1–2 | 195 | 51 |
| 23 | Pima indians diabetes | 1–2 | 768 | 30 |
| 24 | Red wine | 5–6 | 1319 | 3 |
| 25 | Retinopathy | 1–2 | 1151 | 6 |
| 26 | Seeds | 1–2 | 140 | 0 |
| 27 | Seeds | 1–3 | 140 | 0 |
| 28 | Seeds | 2–3 | 140 | 0 |
| 29 | Sonarall | 1–2 | 208 | 7 |
| 30 | Tae | 1–2 | 99 | 1 |
| 31 | Tae | 1–3 | 101 | 3 |
| 32 | Tae | 2–3 | 102 | 2 |
| 33 | Vertebral column 2C | 1–2 | 310 | 35 |
| 34 | Vertebral column 3C | 1–2 | 210 | 43 |
| 35 | Vertebral column 3C | 1–3 | 160 | 25 |
| 36 | Vertebral column 3C | 2–3 | 250 | 20 |
| 37 | White wine | 5–6 | 3655 | 20 |
| 38 | Wine | 1–2 | 130 | 9 |
| 39 | Wine | 1–3 | 107 | 10 |
| 40 | Zoo | 1–2 | 61 | 34 |

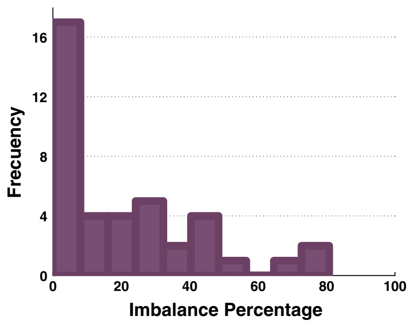

IMBALANCED PROBLEMS

1. The PEP models were trained with balanced problems.
2. The real-world test problems show a varied amount of imbalanced cases.

**Fig. 9** Histogram of imbalance percentage for the 40 real-world classification problems

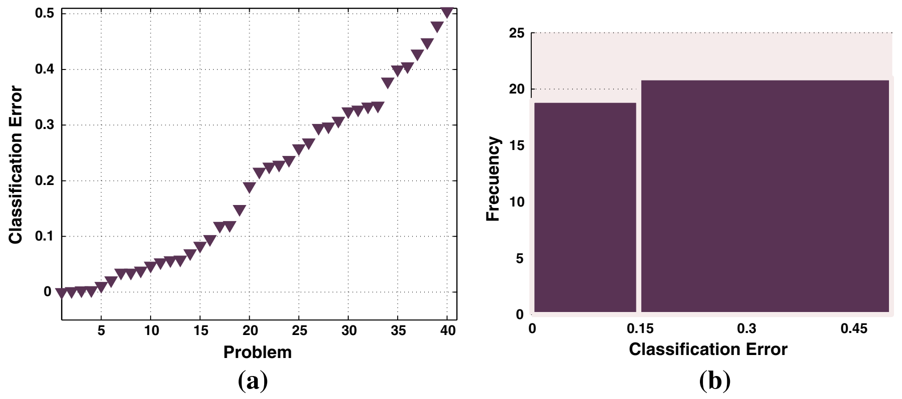

**Fig. 10** Performance of PGPC on the 40 real-world classification problems; where **a** shows the CE$\mu$ for each problem; and **b** shows the histogram over CE$\mu$

coefficient was −0.42 but on real-world problems it is 0.09. In fact, only FE and CD-1 showed a good correlation on both sets.

Table 7 summarizes the performance of the evolved PEPs applied on the real-world problems, showing the median of the RMSE of the best solution found, as well as the RMSE and Pearson's correlation coefficient $\rho$ of the best solution. The table presents three rows of results, one for each feature set (PEP-4F, PEP-5F and PEP-7F). In this case, the best performance is achieved by PEP-4F, which was unexpected. However, if we contrast the results with those achieved on the set of synthetic problems, shown in Table 4, a performance drop-off is evident, based on both median and best performance.

Figure 12 shows three rows of plots, one for each feature set (PEP-4F, PEP-5F and PEP-7F). The figures on the left-hand side column show the PCE of the best PEP model and the true CE$\mu$ for all real-world problems, specifying the RMSE. The

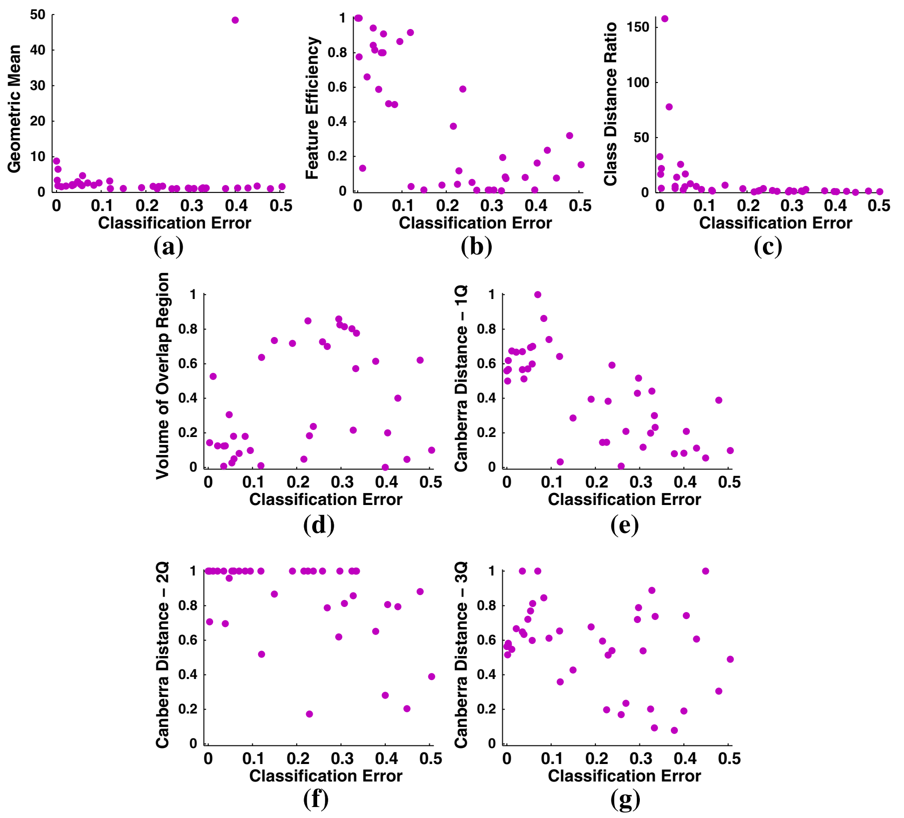

**Fig. 11** Scatter plots show for the real-world problems the relationship between the CE$\mu$ (x-axis) and each descriptive feature (y-axis). **a** SD: $\rho = 0.09$, **b** FE: $\rho = -0.73$, **c** CDR: $\rho = -0.40$, **d** VOR: $\rho = 0.43$, **e** CD-1: $\rho = -0.71$, **f** CD-2: $\rho = -0.46$ and **g** CD-3: $\rho = -0.30$

**Table 7** Prediction performance of the evolved PEPs applied on the real-world problems using each feature set (4F, 5F and 7F, see Table 3)

| | Median RMSE | Best RMSE | Best correlation |
|---|---|---|---|
| *PEP-4F* | **0.1522** | **0.0828** | 0.8634 |
| *PEP-5F* | 0.1583 | 0.0929 | **0.8823** |
| *PEP-7F* | 0.1676 | 0.0930 | 0.8046 |

Performance is given based on the RMSE and Pearson's correlation coefficient, with bold indicating the best performance

figures on the right-hand side column show the CE$\mu$ and PCE as scatter plots, specifying the Pearson's correlation coefficient $\rho$. Again, these figures reveal that the evolved PEP models provide less accurate prediction on real-world problems.

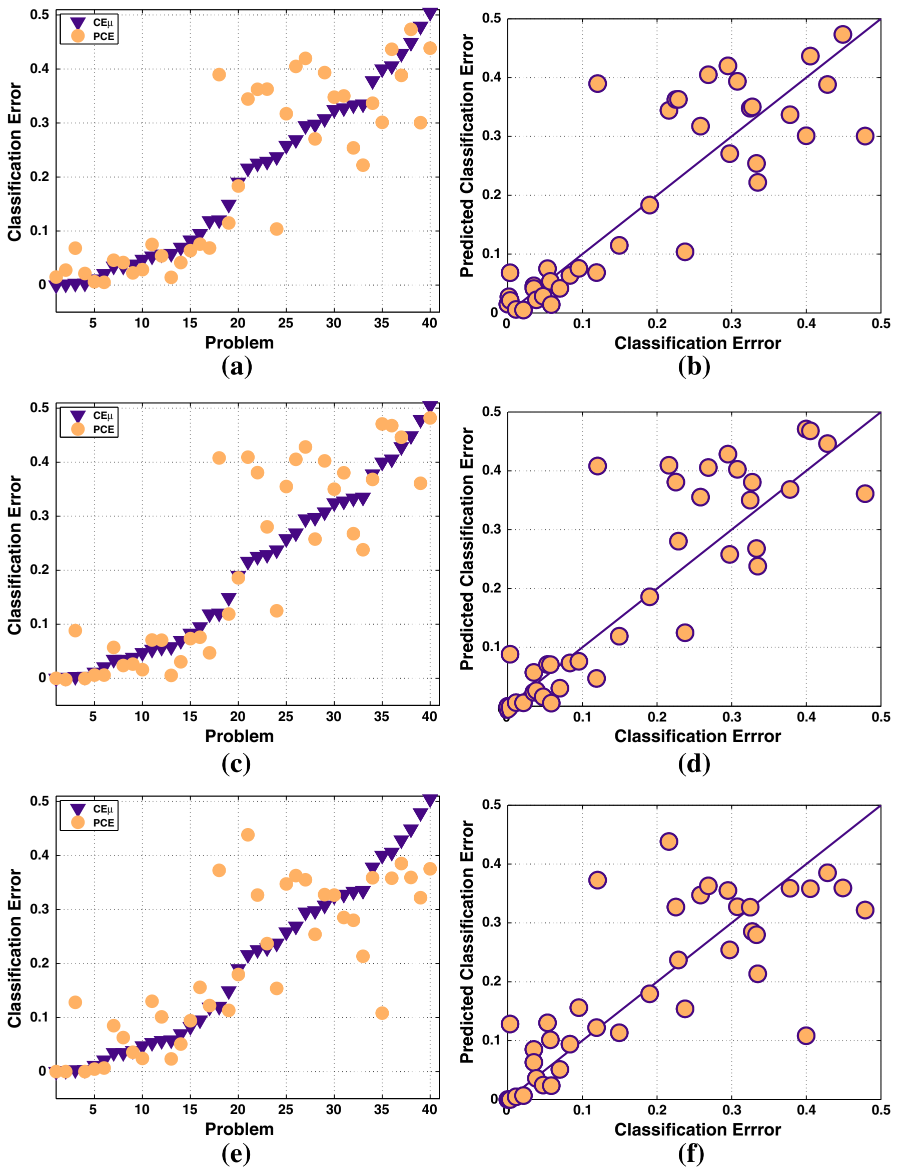

**Fig. 12** Figures show for real-world problems, the performance prediction of the best PEP models evolved with the different feature set, each row belongs to each feature set: PEP-4F (*top*), PEP-5F (*middle*) and PEP-7F (*bottom*). *Plots on the left-hand side column* shows the PCE of the best solution and the known CE$\mu$. The *right-hand side column* shows scatter plots of the PCE and the CE$\mu$. **a** *PEP-4F*: RMSE = 0.0828, **b** *PEP-4F*: $\rho = 0.8634$, **c** *PEP-5F*: RMSE = 0.0929, **d** *PEP-5F*: RMSE = 0.8823, **e** *PEP-7F*: RMSE = 0.0930 and **f** *PEP-7F*: RMSE = 0.8046

## 5 SPEP: specialist predictors of expected performance

The above results are encouraging, but for a real-world application even small improvements in the quality of the predictions could have non-negligible effects. Therefore, in this section we propose an ensemble approach using several PEP models, each one referred to as an SPEP. We propose an ensemble approach for two main reasons. First, previous works suggest that ensemble-based modeling can improve performance in a variety of scenarios [7, 76]. Second, an ensemble approach allows us to obtain two types of predictions, a numerical prediction of expected performance and a categorical or fuzzy prediction based on the chosen ensemble component used to compute the final prediction. The proposal is depicted in Fig. 13, an extension of the basic PEP approach shown in Fig. 1. However, in the SPEP approach before computing the PCE for a given problem, each problem is classified into a specific group using its corresponding feature vector $\beta$. Each group is associated to a particular SPEP in the ensemble, hence if a problem is classified into the $i$th group then the $i$th SPEP is used to compute the predicted PGPC performance on the test set.

To implement this approach, several design choices must be specified. First, how to define a meaningful grouping of problems. Second, train SPEPs that are specialized for each group in order to build the ensemble. Third, chose the correct SPEP for a particular problem by determining its group membership. Each of these issues are discussed next.

### 5.1 Grouping problems based on PGPC performance and training SPEPs

The proposal is to group problems based on the performance of PGPC given by CE$\mu$. This can be seem as a categorical prediction, where problems are grouped into general groups of different difficulty; e.g. easy and hard problems. In particular, we propose two different groupings based on CE$\mu$, using either two or three groups as shown in Fig. 14. The groups were chosen in such a way that the number of (synthetic) problems in each group would be approximately the same, in this way posing a balanced classification task for the SPEP approach. Figure 14 shows the

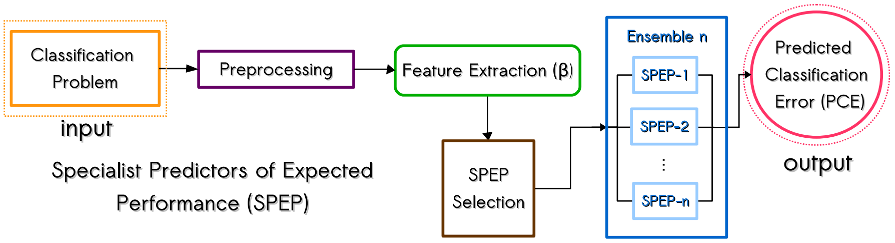

**Fig. 13** Block diagram shows the proposed SPEP approach. The proposed approach is an extension of the basic PEP approach of Fig. 1, with the additional ensemble approach, where problems are first classified into prespecified groups and based on this a corresponding specialized morel (SPEP) is chosen to compute the PCE of PGPC on the test set

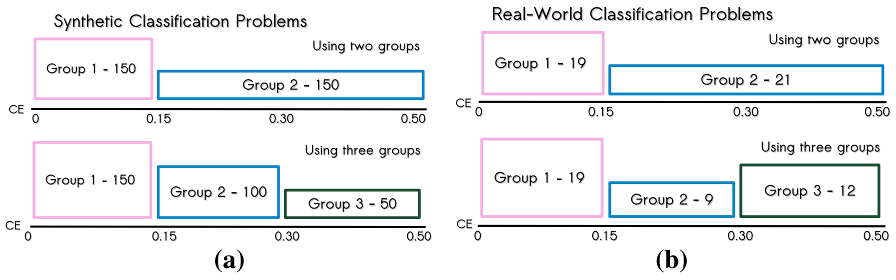

**Fig. 14** The proposed groupings of classification problems used with the SPEP approach, showing the ranges of PGPC performance and the number of problems in each group

ranges of PGPC performance for each group and the number of synthetic problems (Fig. 14a) and real-world problems (Fig. 14b) that fall within each group. The plots on the top divide the problems into two groups, while the plots on the bottom divide the problems into three. Finally, for clarity, since the two group division requires two SPEPs, we refer to a solution for this task as an Ensemble-2, while a solution for the three group task is referred to as an Ensemble-3.

For each group an SPEP is trained using the same strategy described in the previous section for PEPs. Except that instead of using all of the synthetic problems, each SPEP is trained using the subset of synthetic problems from the corresponding group, as depicted in Fig. 14. Since we are interested in presenting the best possible prediction of PGPC performance on real-world problems, we must select the best predictive models. Therefore, the testing phase is performed using two subsets of the real-world problems, one for validation and other for testing.

## 5.2 SPEP selection

As depicted in Fig. 13, in order to choose an SPEP we must first classify each problem to its corresponding group. This is a straightforward classification task, solved using each problem's feature vector $\beta$ as the decision variables. Several classification algorithms are tested [5], namely:

1. Euclidean distance classifier (EDC).
2. Mahalanobis distance classifier (MDC).
3. Naive Bayes classifier (NBC).
4. Support vector machine (SVM), with Gaussian radial basis function kernel and a default scaling factor of 1.
5. K-Nearest Neighbor (KNN), using $K = 5$ neighbors.
6. Treebagger Classifier (TBC), using three trees.
7. Probabilistic Genetic Programming Classifier (PGPC), parameters on Table 1.

Moreover, the classification task is posed using different subsets of the features in $\beta$ as previously described in Table 3. We apply all classifiers using all subsets of features on both the two-group and three-group classification tasks.

As done for the SPEP models, in all cases the complete set of synthetic problems $\mathcal{Q}'$ is used to train the classifiers. The testing phase is performed with two sets, 10 % of the real-world problems are used as a validation set while the remaining 90 % of real-world problems are used for testing. After performing 100 independent runs, the best solution is chosen based on its validation set performance, and methods are compared based on the performance on the testing set. If several solutions achieve the best validation set performance, than the final solution used in the ensemble is randomly chosen.

## 5.3 Evaluation of SPEP ensembles

This section presents the performance of the evolved SPEP models, and the performance of the complete ensembles, using both the true problem groups (an oracle approach, where the correct SPEP is always chosen) and the predicted group by the best classifier (a more realistic testing scenario).

### *5.3.1 Ensemble-2 solutions*

To visualize the underlying difficulty of choosing the correct SPEP for a given problem (i.e., determining the group to which it belongs to) Fig. 15 presents a parallel coordinate plot dividing the problems into two groups, where each coordinate is given by a feature in $\beta$. Plots are shown for synthetic (Fig. 15a) and real-world problems (Fig. 15b). The plots on the left show a single line for each problem, while the plots on the right show the median values for each group. For clarity in the parallel plots, the features SD and CDR were rescaled to values between [0, 1].

Table 8 summarizes the performance of the best SPEP models used to build the Ensemble-2 solution. The first columns specifies the feature subset used from $\beta$. The second column specifies the evaluated SPEP, SPEP-1 was trained with synthetic problems from the first group while SPEP-2 was trained with problems from the second group. The training RMSE is given in column 3. Every SPEP was tested on real-world problems from both groups, to illustrate the performance difference and specialization of each model; this is specified in the forth column. The final column gives the testing RMSE on each group.

The results show that the SPEP models are specialized to their groups, achieving error values below 0.1 when tested using problems from their groups, while performing worse when tested on problems from the other group. In general, performance on testing set is good, particularly if we compare with the results achieved by the PEP models from the preceding section. Finally, performance is similar for all feature sets when considering testing performance, with the best performance on Group 1 achieved by using the set 4F and the best performance on Group 2 with set 5F.

The results in Table 8 represent the best possible performance if the correct problem group is chosen, but also confirm that if the correct group is not chosen than prediction accuracy can decline. Table 9 summarizes the performance of all of

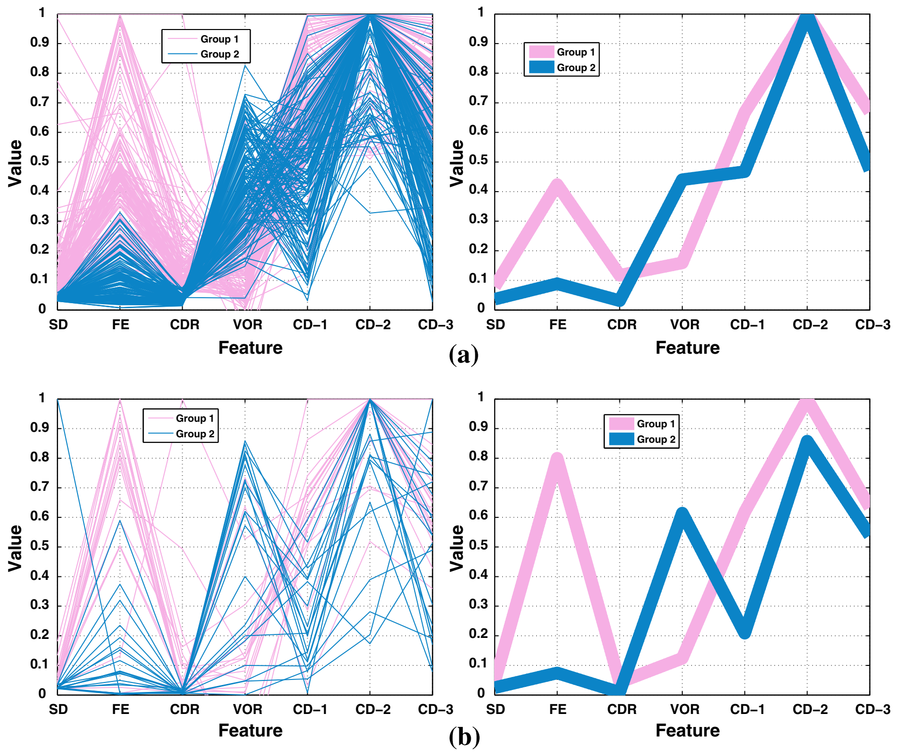

**Fig. 15** Parallel coordinate plots dividing the problems into two groups, where each coordinate is given by a feature in $\beta$. Plots are shown for synthetic (**a**) and real-world problems (**b**). The *plots on the left* show a single line for each problem, while the *plots on the right* show the median values for each group

**Table 8** RMSE of the best evolved SPEP models, using different feature sets (first column)

| | SPEP | Training | Testing group | Testing |
|---|---|---|---|---|
| *4F* | SPEP-1 | 0.0201 | 1 | **0.0315** |
| | | | 2 | 0.2470 |
| | SPEP-2 | 0.0341 | 1 | 0.1445 |
| | | | 2 | 0.0919 |
| *5F* | SPEP-1 | 0.0195 | 1 | 0.0380 |
| | | | 2 | 0.1819 |
| | SPEP-2 | 0.0380 | 1 | 0.1119 |
| | | | 2 | **0.0832** |
| *7F* | SPEP-1 | 0.0212 | 1 | 0.0469 |
| | | | 2 | 0.2096 |
| | SPEP-2 | 0.0332 | 1 | 0.1586 |
| | | | 2 | 0.1014 |

Performance is given based on training and testing set. Moreover, each SPEP-*i* corresponds to the *i*th problem group but is tested on both problem groups, as specified in the fourth column. Bold indicates the best performance on each group

**Table 9** Performance on the SPEP selection problem for all tested classifiers, showing the median classification error from 100 independent runs

| Algorithm | EDC | MDC | NBC | SVM | KNN | TBC | PGPC |
|---|---|---|---|---|---|---|---|
| *4F* | | | | | | | |
| Training | 0.1533 | 0.0567 | 0.0200 | 0.0233 | 0.0133 | 0.0067 | 0.0100 |
| Testing | 0.2500 | 0.1389 | 0.1111 | 0.1111 | 0.1389 | 0.1111 | **0.0833** |
| *5F* | | | | | | | |
| Training | 0.1533 | 0.0567 | 0.0200 | 0.0200 | 0.0200 | 0.0067 | 0.0100 |
| Testing | 0.2778 | 0.1389 | 0.1389 | 0.1389 | 0.1667 | 0.1389 | **0.1111** |
| *7F* | | | | | | | |
| Training | 0.1533 | 0.0467 | 0.0200 | 0.0033 | 0.0200 | 0.0067 | 0.0100 |
| Testing | 0.2778 | 0.1389 | 0.1389 | 0.2500 | 0.1667 | 0.1111 | **0.0972** |

The performance is given on the training and testing sets

Bold text indicates the best performance on each feature set

the tested classifiers for the two-group case, showing the median classification error achieved on the training and testing sets. On these tests, PGPC achieves the best performance based on test error.

Table 10 shows the performance of the best classifier obtained from each method and chosen based on the validation set. In this table performance is given using all real-world problems. Again, PGPC clearly outperforms all other variants, with the best performance achieved using feature set 7F with a classification error of 0.0250.

It is now possible to evaluate the performance of the complete Ensemble-2 solutions, using the best evolved SPEPs and the best classifier. These results are summarized in Table 11, specifying the RMSE and Pearson's correlation coefficient when evaluated on the synthetic and real-world problem sets. These tests show that the Ensemble-2 solutions can achieve low predictive error and a high correlation with the true PGPC performance, for both synthetic and real-world problems. In particular, using feature set 5F correlation on synthetic problems is close to unity, while performance on the real-world problems show the lowest error and approximately 0.9 correlation.

Focusing on the real-world problems, Fig. 16 summarizes the performance of the Ensemble-2 predictors using each feature set (each row of the figure). The column on the left-hand side shows plots of the ground truth CE$\mu$ of each problem

**Table 10** Performance on the SPEP selection problem for all tested classifiers, showing the classification error of the best solution found, evaluated over all real-world problems, with bold indicating the best performance on each feature set

| Feature set | EDC | MDC | NBC | SVM | KNN | TBC | PGPC |
|---|---|---|---|---|---|---|---|
| *4F* | 0.2500 | 0.1250 | 0.1000 | 0.1000 | 0.1250 | 0.1250 | **0.0500** |
| *5F* | 0.2750 | 0.1250 | 0.1250 | 0.1250 | 0.1500 | 0.1250 | **0.1000** |
| *7F* | 0.2750 | 0.1250 | 0.1250 | 0.2500 | 0.1500 | 0.1250 | **0.0250** |

**Table 11** Ensemble-2 prediction accuracy using each feature set (4F, 5F and 7F), using the best evolved SPEPs and the best classifiers with each feature set

| Feature set | Synthetic | | Real-world | |
|---|---|---|---|---|
| | RMSE | Correlation | RMSE | Correlation |
| *4F* | 0.0284 | 0.9709 | 0.0818 | 0.8717 |
| *5F* | 0.0302 | **0.9984** | **0.0736** | **0.8981** |
| *7F* | **0.0276** | 0.9728 | 0.0897 | 0.8514 |

Performance is given based on the RMSE and Pearson's correlation coefficient when evaluated on the synthetic and real-world problem sets; with *bold* indicating the best performance on real-world problems

(triangles) and the Ensemble-2 PCE. These plots show three types of PCE: (1) correctly classified problems for which the appropriate SPEP was selected (CC-PCE); (2) misclassified problems for which an incorrect SPEP was selected (MC-PCE); and (3) for the misclassified problems the oracle SPEP prediction (O-PCE), which is the PCE produced by the correct SPEP. The column on the right-hand side of Fig. 16 presents scatter plots of the true CE$\mu$ and the PCE, using the same notation.

These plots provide a graphical confirmation of the quality of the performance prediction. It is important to highlight the impact of a misclassified problem, shown as a black circle, compared to the prediction on the same problem if the correct SPEP had been chosen (O-PCE). For all problems for which the correct SPEP was chosen the PCE is highly correlated with the ground truth with only marginal differences in most cases.

### 5.3.2 *Ensemble-3 solutions*

Figure 17 presents a parallel coordinate plot dividing the problems into three groups, where each coordinate is given by a feature in $\beta$. Plots are shown for synthetic (Fig. 17a) and real-world problems (Fig. 17b). The plots on the left show a single line for each problem, while the plots on the right show the median values for each group. For clarity, features SD and CDR were rescaled to values between [0, 1].

Table 12 summarizes the performance of the best SPEP models used to build the Ensemble-3 solution. The first column, from left to right, specifies the feature subset used from $\beta$. The second column specifies the evaluated SPEP, SPEP-1 was trained with synthetic problems from the first group, SPEP-2 with problems from the second group and SPEP-3 with problems from the third group. The third column shows the training RMSE, the fourth column shows the testing group and the final columns shows the testing RMSE.

Again, the results show that the SPEP models are specialized to their respective groups. Performance on the testing set is better than the simple PEP models, but worse than the Ensemble-2 solution presented before. All feature sets produce similar performance on testing set problems, with the best performance on Group 1

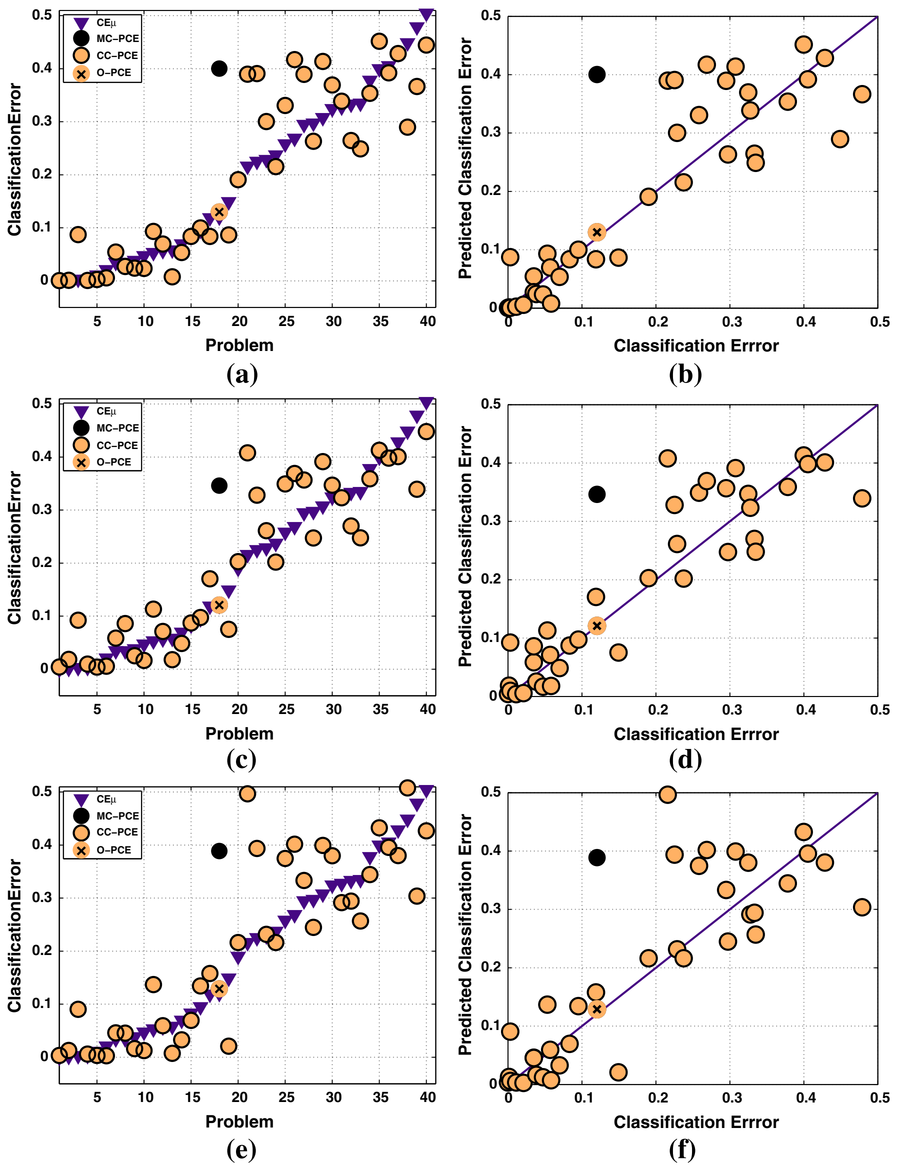

**Fig. 16** Performance prediction of the best Ensemble-2 solutions for each feature set: 4F (*top*), 5F (*middle*) and 7F (*bottom*). The *left-hand side column of plots* show the ground truth CE$\mu$ of each problem (*triangles*) and the corresponding PCE (*circles*). The *right-hand side column* shows scatter plots between the CE$\mu$ and the corresponding PCE. The PCE is presented in three different cases: the PCE of a correctly classified problem (CC-PCE, *circle*); the PCE of a misclassified problem (MC-PCE, *dark circle*); and the oracle PCE of a misclassified problem using the correct SPEP (O-PCE, *circle with a cross*). **a** *4F*: RMSE = 0.0818, **b** *4F*: $\rho = 0.8717$, **c** *5F*: RMSE = 0.0736, **d** *5F*: $\rho = 0.8981$, **e** *7F*: RMSE = 0.0897 and **f** *7F*: $\rho = 0.8514$

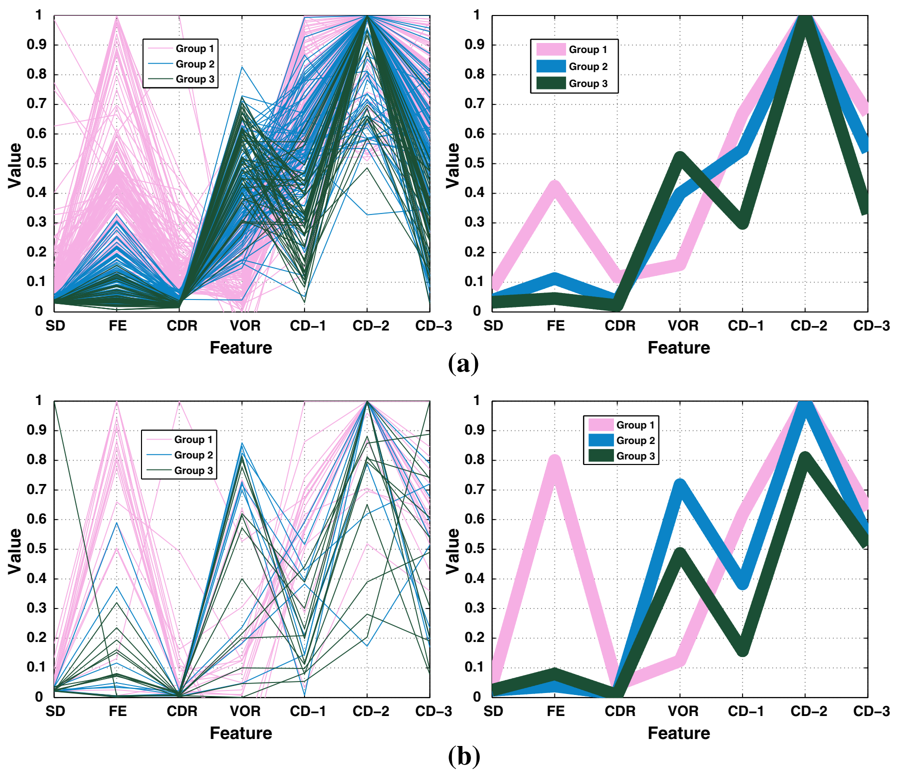

**Fig. 17** Parallel coordinate plots dividing the problems into three groups, where each coordinate is given by a feature in $\beta$. Plots are shown for synthetic (**a**) and real-world problems (**b**). The *plots on the left* show a single line for each problem, while the *plots on the right* show the median values for each group

and Group 2 achieved by using set 4F, and the best performance on Group 3 with set 5F.

The results summarized in Table 12 represent the best possible performance if the correct problem group is chosen, but also confirm that if the correct group is not chosen than prediction accuracy can decline. Table 13 summarizes the performance of all of the tested classifiers for the three-group case, showing the median classification error achieved on the training and testing sets. On these tests, TBC achieves the best median performance. Table 14 focuses on the performance of the best classifier evaluated over all real-world problems. Again, TBC outperforms all other variants, with the best performance achieved using feature set 5F with a classification error of 0.1750.

It is now possible to evaluate the performance of the complete Ensemble-3 solutions, using the best evolved SPEPs and the best classifier. These results are summarized in Table 15, specifying the RMSE and Pearson's correlation coefficient when evaluated on the synthetic (training) and real-world (validation and testing) problem sets. These tests show that the Ensemble-3 solutions can achieve low predictive error and a high correlation with the true PGPC performance, for both

**Table 12** RMSE of the best evolved SPEP models, using different feature sets (first column)

| SPEP | Training | Testing group | Testing |
|---|---|---|---|
| *4F* | | | |
| SPEP3-1 | 0.0201 | 1 | **0.0315** |
| | | 2 | 0.1312 |
| | | 3 | 0.2767 |
| SPEP3-2 | 0.0303 | 1 | 0.1883 |
| | | 2 | **0.0302** |
| | | 3 | 0.1459 |
| SPEP3-3 | 0.0264 | 1 | 0.3955 |
| | | 2 | 0.1349 |
| | | 3 | 0.0532 |
| *5F* | | | |
| SPEP3-1 | 0.0195 | 1 | 0.0380 |
| | | 2 | 0.2076 |
| | | 3 | 0.1602 |
| SPEP3-2 | 0.0313 | 1 | 0.0931 |
| | | 2 | 0.0380 |
| | | 3 | 0.1245 |
| SPEP3-3 | 0.0294 | 1 | 0.2691 |
| | | 2 | 0.1250 |
| | | 3 | **0.0525** |
| *7F* | | | |
| SPEP3-1 | 0.0212 | 1 | 0.0469 |
| | | 2 | 0.1723 |
| | | 3 | 0.2391 |
| SPEP3-2 | 0.0285 | 1 | 0.1096 |
| | | 2 | 0.0352 |
| | | 3 | 0.1719 |
| SPEP3-3 | 0.0277 | 1 | 0.1339 |
| | | 2 | 0.1133 |
| | | 3 | 0.0531 |

Performance is given based on training and testing set. Moreover, each SPEP-*i* corresponds to the *i*th problem group but is tested on all problem groups, as specified in column 4

Bold text indicates best performance on each group

synthetic and real-world problems. In all feature sets the correlation on synthetic problems is above 0.97, while the best performance on the real-world problems is achieved using set 5F based on RMSE and set 7F based on correlation.

Focusing on the real-world problems, Fig. 18 summarizes the performance of the Ensemble-3 predictors using each feature set (each row of the figure). These plots illustrate the performance of the achieved prediction. As in the Ensemble-2 case, it is important to highlight the impact of misclassified problems (shown as a black circle) compared to the prediction on the same problem if the correct SPEP had been chosen (O-PCE). In this case we can see more misclassifications. The reason is evident in Fig. 17, since Group 2 and Group 3 are not so easily differentiated. However, the impact of the misclassified problems is not as large as it is for the

**Table 13** Performance on the SPEP selection problem for all tested classifiers, showing the median classification error from 100 independent runs

| Algorithm | EDC | MDC | NBC | SVM | KNN | TBC | PGPC |
|---|---|---|---|---|---|---|---|
| *4F* | | | | | | | |
| Training | 0.2533 | 0.1967 | 0.0833 | 0.1067 | 0.0467 | 0.0167 | 0.0633 |
| Testing | 0.4722 | 0.3056 | 0.3889 | 0.3611 | 0.3056 | **0.2778** | 0.3611 |
| *5F* | | | | | | | |
| Training | 0.2500 | 0.1933 | 0.0833 | 0.1033 | 0.0533 | 0.0200 | 0.0667 |
| Testing | 0.5000 | **0.3056** | 0.4167 | 0.3611 | 0.3333 | **0.3056** | 0.3333 |
| *7F* | | | | | | | |
| Training | 0.2467 | 0.1867 | 0.0800 | 0.0533 | 0.0567 | 0.0167 | 0.0667 |
| Testing | 0.5000 | **0.3056** | 0.3889 | 0.4444 | 0.3333 | 0.3333 | 0.3333 |

The performance is given on the training and testing sets, with bold indicating the best performance on each feature set

**Table 14** Performance on the SPEP selection problem for all tested classifiers, showing the classification error of the best solution found, evaluated over all real-world problems, with bold indicating the best performance on each feature set

| Feature set | EDC | MDC | NBC | SVM | KNN | TBC | PGPC |
|---|---|---|---|---|---|---|---|
| *4F* | 0.4750 | 0.3000 | 0.4000 | 0.3500 | 0.3000 | **0.2250** | 0.2500 |
| *5F* | 0.5000 | 0.3000 | 0.4250 | 0.3500 | 0.3250 | **0.1750** | 0.2500 |
| *7F* | 0.5000 | 0.3000 | 0.3750 | 0.4500 | 0.3250 | **0.2500** | 0.3000 |

**Table 15** Ensemble-3 prediction accuracy using each feature set (4F, 5F and 7F), using the best evolved SPEPs and the best classifiers with each feature set

| Feature set | Synthetic | | Real-world | |
|---|---|---|---|---|
| | RMSE | Correlation | RMSE | Correlation |
| *4F* | 0.0288 | 0.9704 | 0.0808 | 0.8685 |
| *5F* | 0.0300 | 0.9687 | **0.0775** | 0.8707 |
| *7F* | **0.0285** | **0.9714** | 0.0786 | **0.8736** |

Performance is given based on the RMSE and Pearson's correlation coefficient when evaluated on the synthetic and real-world problem sets; with bold indicating the best performance on real-world problems

Ensemble-2 solution, given the comparatively similar RMSE of both the Ensemble-3 and the Ensemble-2 solutions.

## 6 Discussion

This work presents three approaches towards solving the performance prediction problem using the general PEP approach: a single PEP, an Ensemble-2 solution (2 SPEPs) and an Ensemble-3 solution (3 SPEPs). Table 16 presents a comparison of

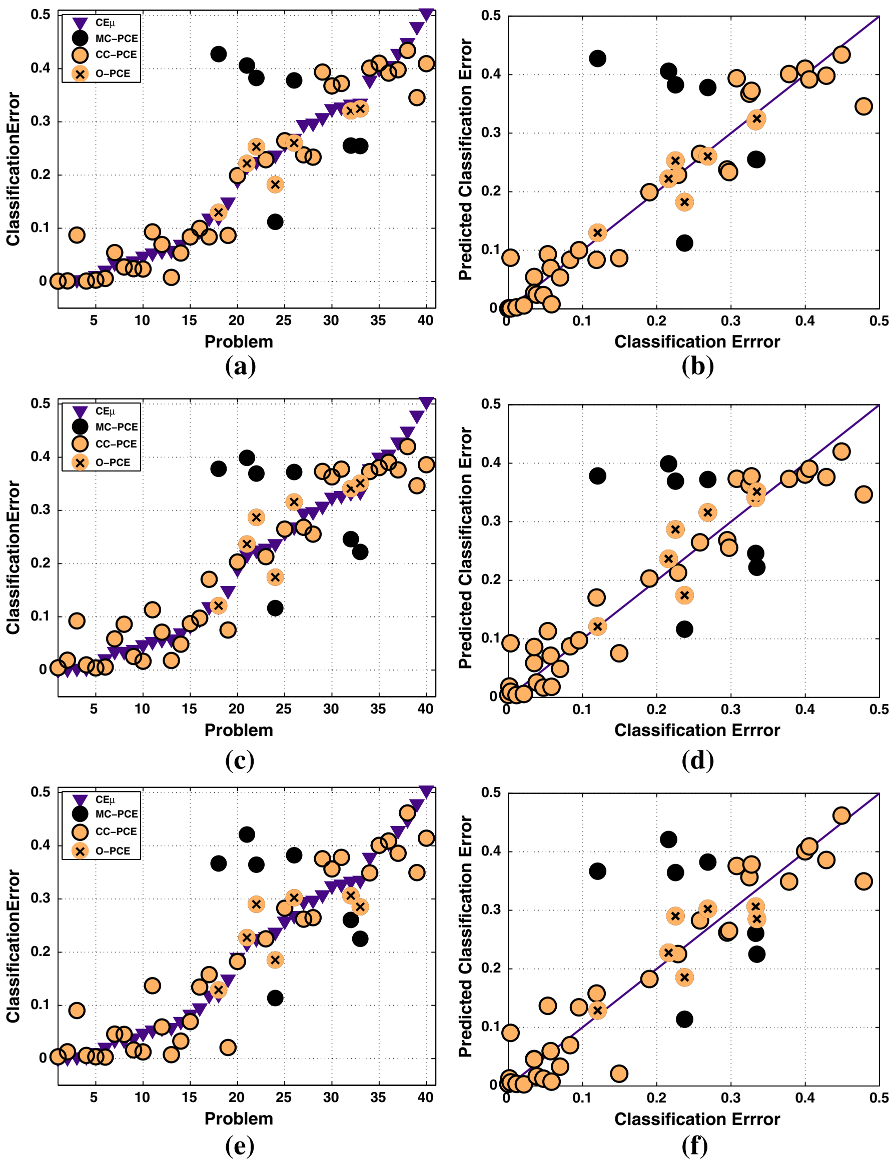

**Fig. 18** Performance prediction of the best Ensemble-3 solutions for each feature set: 4F (*top*), 5F (*middle*) and 7F (*bottom*). The *left-hand side column of plots* show the ground truth CE$\mu$ of each problem (*triangles*) and the corresponding PCE (*circles*). The *right-hand side column* show scatter plots between the CE$\mu$ and the corresponding PCE. The PCE is presented in three different cases: the PCE of a correctly classified problem (CC-PCE, *circle*); the PCE of a misclassified problem (MC-PCE, *dark circle*); and the oracle PCE of a misclassified problem using the correct SPEP (O-PCE, *circle with a cross*). **a** *4F*: RMSE = 0.0808, **b** *4F*: $\rho = 0.8685$, **c** *5F*: RMSE = 0.0775, **d** *5F*: $\rho = 0.8707$, **e** *7F*: RMSE = 0.0786 and **f** *7F*: $\rho = 0.8736$

**Table 16** A comparison of each predictor approach; where bold indicates best performance

| | PEP | | SPEP Ensemble-2 | | SPEP Ensemble-3 | |
|---|---|---|---|---|---|---|
| | RMSE | Correlation | RMSE | Correlation | RMSE | Correlation |
| *4F* | 0.0828 | 0.8634 | 0.0818 | 0.8717 | 0.0808 | 0.8685 |
| *5F* | 0.0929 | 0.8823 | **0.0736** | **0.8981** | 0.0775 | 0.8707 |
| *7F* | 0.0930 | 0.8046 | 0.0897 | 0.8514 | 0.0786 | 0.8736 |

the best results of each solution evaluated on the real-world test cases. While all solutions achieve comparable results, it is clear that the Ensemble-2 solution achieves the lowest RMSE and the highest correlation, particularly when using set 5F. These results provide two important insights. First, that the ensemble approach is justified in this domain, with both ensembles outperforming the single PEP models. Second, that grouping the problem into useful subsets based on performance can be solved using two broad categories, what might be considered as *easy* and *difficult* problems. However, differentiating problems further becomes difficult given the underlying distribution of problems within feature space, as shown in Fig. 17 and confirmed by the lower performance of the Ensemble-3 solution.

Before concluding let us discuss some additional observations, starting with the relative importance of each feature used to predict performance. Since all PEPs and SPEPs where generated using symbolic regression with GP, we use statistics over the GP runs to measure the importance of each feature. Figure 19 shows two plots that quantify the frequency of feature use when the models were evolved using the complete feature set (7F) over 100 independent runs. Figure 19a is a bar plot where the frequency is given by summing the number of times that each feature appeared as a terminal element in the best symbolic regression solutions from each run. Figure 19b plots the median of the number of times that each feature appears in the best solution from each run. In this plot each line corresponds to either a single PEP or a particular SPEP from each ensemble; for instance, for the Ensemble-2 solutions there are two SPEPs labeled as Ensemble-2-1 and Ensemble-2-2, and similarly for the Ensemble-3 models. Notice that in this plot the lines for SPEP Ensemble-2-1 and SPEP Ensemble-3-1 overlap since they correspond to the same problem group.

Figure 19 reveals some interesting facts of how the symbolic regression system performs feature selection. As shown in Fig. 9, the features with higher correlation to PGPC performance are FE, VOR, CDR and CD-1, in that order. However, if we consider all evolved models (Fig. 19a) FE is not the most widely used feature, the evolved models consistently select VOR and CDR at a higher frequency. On the other hand, the less correlated features SD, CD-2 and CD-3 are indeed used less by GP.

If we consider feature frequency in finer detail by comparing the frequency in the PEP models with the frequency in each SPEP, some interesting trends appear, as shown in Fig. 17b. In this case it is clear that some features are better predictors of PGPC performance on particular problem groups. For instance, CDR and VOR are

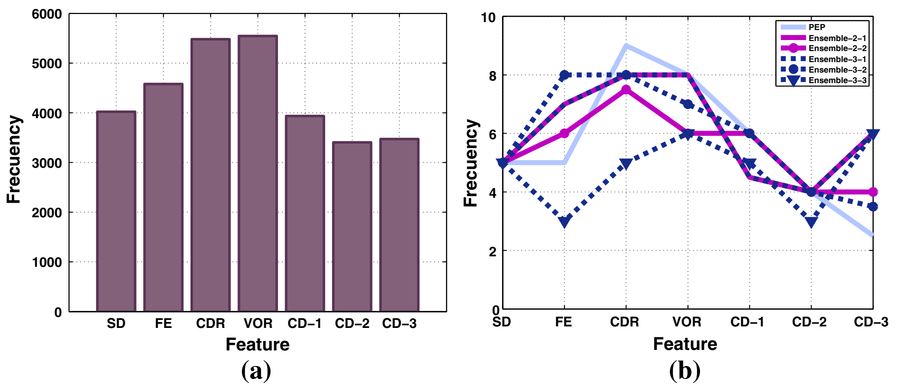

**Fig. 19** Feature selection by the symbolic regression GP used to evolve all PEP and SPEP models, showing usage frequency over 100 runs: **a** *bar plot* of the total number of times that each feature appeared as a terminal element in the best models; and **b** median of the number of times that each feature appeared in each tree. **a** *4F*: RMSE = 0.0808, **b** *4F*: $\rho = 0.8685$, **c** *5F*: RMSE = 0.0775, **d** *5F*: $\rho = 0.8707$, **e** *7F*: RMSE = 0.0786 and **f** *7F*: $\rho = 0.8736$. **a***7F* and **b** *7F*

the most used by the PEP models. On the other hand, FE is used with a higher frequency when predicting performance on easier problems (Ensemble-2-1, Ensemble-3-1) than for the hardest problems (Ensemble-3-3). This is also the case for CDR and slightly for CD-2. Conversely, while CD-3 is rarely used in PEP models, it appears to be very useful in predicting performance on the most difficult problems (Ensemble-3-3) and the easiest (Ensemble-2-1 and Ensemble-3-1) problems.

It is also instructive to determine if the dimensionality reduction applied as preprocessing has a negative effect with regards to performance prediction. Our proposal is to use the first two principal components of the data, in order to simplify the description of the real-world problems. However, it is not clear if the percentage of the variance described by such few components is enough to properly characterize the problems. To analyze this, Fig. 20 presents scatter plots of all the real-world problems $p \in \mathcal{Q}'$, showing the percentage of the total variance of the data explained by the first two principal components (x-axis) and the prediction error (PE) (y-axis) computed as the absolute difference between CE$\mu$ and PCE. In particular, Fig. 20a is based on the PEP-4F model while Fig. 20b is based on the SPEP-2-5F model. The caption of the figure specifies the computed Pearson's correlation coefficient $\rho$ between both measures. Notice that there is no significant correlation, suggesting that the accuracy of the models does not suffer from the proposed preprocessing.

Finally, an implicit goal of the PEP and SPEP models is to obtain accurate performance predictions in a fraction of the time required to obtain those same estimates by actually performing the GP runs. Pragmatically, one way to validate if this goal is achieved is to calculate the running time for all problems, based on the employed PGPC implementation and the complete SPEP process. These experiments were conducted using MATLAB r2013a and the GPLAB toolbox [49]

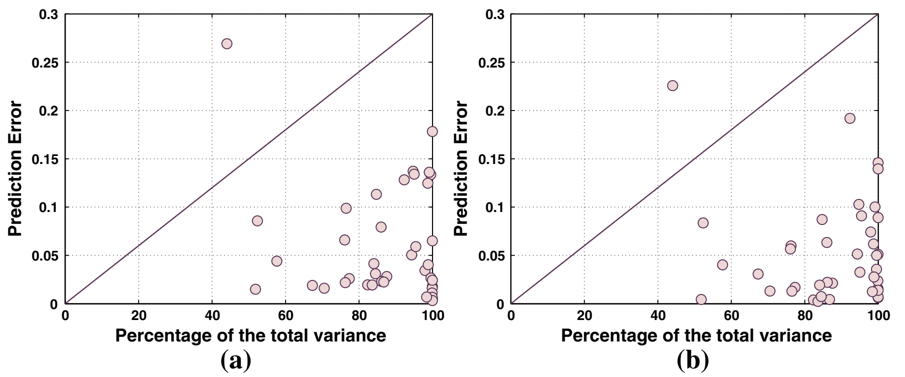

**Fig. 20** Scatter plots show the relationship between the percentage of the total variance explained by two principal components (x-axis) and the prediction error (y-axis), for all problems $p \in Q'$, where the prediction error is the absolute difference between the CE$\mu$ and PCE, figure on the left show the PEP-4F model and figure on the right SPEP-2-5F, where $\rho$ specifies Pearson's correlation coefficient. **a** PEP-4F: $\rho = -0.16$ and **b** SPEP-2-5F: $\rho = -0.08$

running on a PC with Ubuntu 12.04 LTS using an Intel RXeon(R) CPU E3-1270 v3 @ 3.50 GHz $\times$ 8 processor with 15.6 GB of RAM. In these tests, the minimum amount of time required to compute CE$\mu$ (30 runs of PGPC) was 3360.96 seconds, while the maximum amount of time required to compute the PCE (running the SPEP process) was 11.22 seconds. These results clearly show that PEP and SPEP models can be used in real-world scenarios to obtain both accurate and efficient estimations of GP performance.[2]

## 7 Conclusions

This work presents three main contributions. First, extensions of the PEP approach originally proposed in [57, 59, 60], by adding new descriptive measures and testing the PEP models built with synthetic classification problems over a more challenging scenario, performance prediction on real-world classification problems with different dimensions and class imbalance. To achieve the latter we included a preprocessing step for dimensionally reduction, something that previous proposals lacked. Second, the proposed models predict the performance of the GP classifier when they are evaluated on the test set of fitness cases, while previous works focused on predicting training performance. For real-world scenarios, predicting the test performance of a learning algorithm is more relevant since overfitting can appear on difficult problem instances. Third, this work presents a new proposal using an ensemble of SPEPs, where the problems are separated into groups and

[2] It is important to state that our PGPC and SPEP implementations were not implemented in any optimal way, and that running times with other implementations might be substantially different. Nonetheless, we believe that these results give a sufficiently accurate estimate of the possible usefulness of our proposed methodology.

specialized models were built for each group, improving the prediction accuracy on unseen real-world problems.

The main conclusions derived from this work are the following. First, the proposed dimensionality reduction was successful, it allowed the system to learn the predictive models using simple 2D synthetic problems and apply them on real-world problems with considerably more dimensions. Second, the evolved PEP and SPEP models were able to accurately predict PGPC performance on imbalanced datasets, without the need of using imbalanced data during the training phase. Third, the new descriptive measures proposed in this work (CD-1, CD-2, CD-3) complemented the problem descriptors used in previous works to help improve predictive accuracy. Some of the proposed descriptors (CD-1) were among the most correlated with PGPC performance; their usefulness was confirmed when analyzing the feature selection performed by GP. However, it's important to note that all descriptors were used in most evolved PEPs, even if some descriptors exhibited very small amounts of correlation with PGPC performance. Finally, our ensemble proposal provides two general perspectives of the prediction task: categorical and numerical prediction. Where, a categorical prediction is used to select specific SPEPs, while the numerical prediction is given by the chosen SPEP. While not explored in this work, the categorical prediction might be sufficient for some applications, such as in fuzzy inference systems.

Finally, possibles future work derived from this research includes the following. The problem descriptors used in this work produced good results, but defining the optimal set of descriptors is still an open question. We will also use this methodology for many classifiers, deriving one PEP for each classifier, thus allowing us to create an expert system for classifier selection. Another possibility is to use the PEPs within a wrapper approach, where the PEP model could be used as a surrogate fitness function for GP-based classifiers. Moreover, these methodologies could be extended to predict the performance of a GP-based symbolic regression system, building PEP models using a set of descriptive measures that can characterize symbolic regression problems accurately. To do so, a proper dimensionality reduction step must be developed.

**Acknowledgments** This research was supported by CONACYT Basic Science Research Project No. 178323, TecNM (México) Research Project 5621.15-P, and by the FP7-Marie Curie-IRSES 2013 European Commission program through project ACoBSEC with Contract No. 612689. First author was supported by CONACYT doctoral Scholarship No. 226981. The fourth author acknowledges funding provided by an ELEVATE Fellowship, the Irish Research Council's Career Development Fellowship co-funded by Marie Curie Actions, and thanks the TAO group at INRIA Saclay and LRI—Univ. Paris-Sud and CNRS, Orsay, France for hosting him during the outgoing phase of the ELEVATE Fellowship.

## References

1. L. Altenberg, *The Evolution of Evolvability in Genetic Programming* (MIT Press, Cambridge, 1994)
2. L. Altenberg, Fitness distance correlation analysis: an instructive counterexample, in *Proceedings of the Seventh International Conference on Genetic Algorithms* (Morgan Kaufmann, Los Altos, 1997), pp. 57–64

3. P.J. Bentley, Evolutionary, my dear Watson Investigating Committee-based Evolution of Fuzzy Rules for the Detection of Suspicious Insurance Claims, in *Genetic and Evolutionary Computation Conference (GECCO-2000)* (2000), pp. 702–709
4. M. Clergue, P. Collard, M. Tomassini, L. Vanneschi, Fitness distance correlation and problem difficulty for genetic programming, in *GECCO 2002: Proceedings of the Genetic and Evolutionary Computation Conference, New York, USA* (2002), pp. 724–732
5. R.O. Duda, P.E. Hart, D.G. Stork, *Pattern Classification*, 2nd edn. (Wiley, London, 2000)
6. A.E. Eiben, J.E. Smith, *Introduction to Evolutionary Computing* (Springer, Berlin, 2003)
7. G. Folino, C. Pizzuti, G. Spezzano, An ensemble-based evolutionary framework for coping with distributed intrusion detection. Genet. Program Evol. Mach. **11**(2), 131–146 (2010)
8. E. Galván-López, S. Dignum, R. Poli, The effects of constant neutrality on performance and problem hardness in gp, in *Proceedings of the 11th European Conference on Genetic Programming*, EuroGP'08 (Springer, Berlin, 2008), pp. 312–324
9. E. Galván-López, J. McDermott, M. O'Neill, A. Brabazon, Defining locality in genetic programming to predict performance, in *IEEE Congress on Evolutionary Computation* (2010), pp. 1–8
10. E. Galván-López, J. McDermott, M. O'Neill, A. Brabazon, Defining locality as a problem difficulty measure in genetic programming. Genet. Program Evol. Mach. **12**(4), 365–401 (2011)
11. E. Galván-López, R. Poli, An empirical investigation of how and why neutrality affects evolutionary search, in *Proceedings of the 8th Annual Conference on Genetic and Evolutionary Computation*, GECCO '06 (ACM, New York, 2006), pp. 1149–1156
12. E. Galván-López, R. Poli, Some steps towards understanding how neutrality affects evolutionary search, in *Parallel Problem Solving from Nature—PPSN IX*, vol. 4193, Lecture Notes in Computer Science, ed. by T. Runarsson, H.G. Beyer, E. Burke, J. Merelo-Guervós, L. Whitley, X. Yao (Springer, Berlin, 2006), pp. 778–787
13. D.E. Goldberg, Simple genetic algorithms and the minimal, deceptive problem, in *Genetic Algorithms and Simulated Annealing, Research Notes in Artificial Intelligence*, ed. by L. Davis (Pitman, London, 1987), pp. 74–88
14. M. Graff, H.J. Escalante, J. Cerda-Jacobo, A.A. Gonzalez, Models of performance of time series forecasters. Neurocomputing 122(0), 375–385 (2013). Advances in Cognitive and Ubiquitous Computing Selected Papers from the Sixth International Conference on Innovative Mobile and Internet Services in Ubiquitous Computing (IMIS-2012)
15. M. Graff, R. Poli, Practical model of genetic programming's performance on rational symbolic regression problems, in *EuroGP* (2008), pp. 122–133
16. M. Graff, R. Poli, Practical performance models of algorithms in evolutionary program induction and other domains. Artif. Intell. **174**(15), 1254–1276 (2010)
17. M. Graff, R. Poli, Performance models for evolutionary program induction algorithms based on problem difficulty indicators, in *Proceedings of the 14th European Conference on Genetic Programming*, EuroGP'11 (Springer, Berlin, Heidelberg, 2011), pp. 118–129
18. M. Graff, R. Poli, J.J. Flores, Models of performance of evolutionary program induction algorithms based on indicators of problem difficulty. Evol. Comput. **21**(4), 533–560 (2013)
19. H. Guo, L. Jack, A. Nandi, Feature generation using genetic programming with application to fault classification. IEEE Trans. Syst. Man Cybern. Part B Cybern. **35**(1), 89–99 (2005)
20. J. He, T. Chen, X. Yao, On the easiest and hardest fitness functions. IEEE Trans. Evol. Comput. **19**(2), 295–305 (2015)
21. S. Hengpraprohm, P. Chongstitvatana, A genetic programming ensemble approach to cancer microarray data classification, in *3rd International Conference on Innovative Computing Information and Control, 2008. ICICIC '08* (2008), pp. 340–340
22. T.K. Ho, M. Basu, Complexity measures of supervised classification problems. IEEE Trans. Pattern Anal. Mach. Intell. **24**(3), 289–300 (2002)
23. K. Imamura, T. Soule, R. Heckendorn, J. Foster, Behavioral diversity and a probabilistically optimal GP ensemble. Genet. Program Evol. Mach. **4**(3), 235–253 (2003)
24. T. Jones, S. Forrest, Fitness distance correlation as a measure of problem difficulty for genetic algorithms, in *Proceedings of the 6th International Conference on Genetic Algorithms* (Morgan Kaufmann Publishers Inc., San Francisco, 1995), pp. 184–192
25. S. Kauffman, S. Levin, Towards a general theory of adaptive walks on rugged landscapes. J. Theor. Biol. **128**(1), 11–45 (1987)
26. M. Kimura, *The Neutral Theory of Molecular Evolution* (Cambridge University Press, Cambridge, 1983)

27. K.E. Kinnear, Fitness landscapes and difficulty in genetic programming, in *Proceedings of the First IEEE Conference on Evolutionary Computing* (IEEE Press, Piscataway, 1994), pp. 142–147
28. S.B. Kotsiantis, I.D. Zaharakis, P.E. Pintelas, Machine learning: a review of classification and combining techniques. Artif. Intell. Rev. **26**(3), 159–190 (2006)
29. J.R. Koza, *Genetic Programming: On the Programming of Computers by Means of Natural Selection* (MIT Press, Cambridge, 1992)
30. W.B. Langdon, R. Poli, *Foundations of Genetic Programming* (Springer, Berlin, 2002)
31. M. Lichman, UCI machine learning repository (2013) http://archive.ics.uci.edu/ml
32. K. Malan, A.P. Engelbrecht, Particle swarm optimisation failure prediction based on fitness landscape characteristics, in *2014 IEEE Symposium on Swarm Intelligence, SIS 2014, Orlando, FL, USA* (2014), pp. 149–157
33. K.M. Malan, A.P. Engelbrecht, A survey of techniques for characterising fitness landscapes and some possible ways forward. Inf. Sci. **241**, 148–163 (2013)
34. Y. Martínez, L. Trujillo, E. Galván-López, P. Legrand, A comparison of predictive measures of problem difficulty for classification with genetic programming, in *ERA 2012* (Tijuana, Mexico, 2012)
35. K. McClymont, D. Walker, M. Dupenois, The lay of the land: a brief survey of problem understanding, in *Proceedings of the Fourteenth International Conference on Genetic and Evolutionary Computation Conference Companion*, GECCO Companion '12 (ACM, New York, 2012), pp. 425–432
36. N. McPhee, B. Ohs, T. Hutchison, Semantic building blocks in genetic programming, in *Genetic Programming, Lecture Notes in Computer Science*, ed. by M. O'Neill, L. Vanneschi, S. Gustafson, A. Esparcia Alcázar, I. De Falco, A. Della Cioppa, E. Tarantino, vol. 4971 (Springer, Berlin, 2008), pp. 134–145
37. D. Michie, D.J. Spiegelhalter, C.C. Taylor, J. Campbell (eds.), *Machine Learning, Neural and Statistical Classification* (Ellis Horwood, Upper Saddle River, 1994)
38. A. Moraglio, K. Krawiec, C.G. Johnson, Geometric semantic genetic programming, in *Parallel Problem Solving from Nature—PPSN XII—12th International Conference, Taormina, Italy, September 1–5, 2012, Proceedings, Part I* (2012), pp. 21–31
39. M. Muharram, G. Smith, Evolutionary constructive induction. IEEE Trans. Knowl. Data Eng. **17**(11), 1518–1528 (2005)
40. L. Muñoz, S. Silva, L. Trujillo, in *M3GP—multiclass classification with GP*. Genetic programming—18th European conference, EuroGP 2015, Copenhagen, Denmark, April 8–10, 2015, Proceedings (2015), pp. 78–91
41. M. O'Neill, L. Vanneschi, S. Gustafson, W. Banzhaf, Open issues in genetic programming. Genet. Program Evol. Mach. **11**(3–4), 339–363 (2010)
42. R. Poli, E. Galván-López, The effects of constant and bit-wise neutrality on problem hardness, fitness distance correlation and phenotypic mutation rates. IEEE Trans. Evol. Comput. **16**(2), 279–300 (2012)
43. R. Poli, M. Graff, N.F. McPhee, Free lunches for function and program induction, in *Proceedings of the tenth ACM SIGEVO workshop on foundations of genetic algorithms*, FOGA '09 (ACM, New York, 2009), pp. 183–194
44. B. Punch, D. Zongker, E. Goodman, Advances in genetic programming, in *The Royal Tree Problem, a Benchmark for Single and Multiple Population Genetic Programming* (MIT Press, Cambridge, 1996), pp. 299–316
45. C. Qing-Shan, G.G. De-fu, W. Li-Jun, C. Huo-Wang, A modified genetic programming for behavior scoring problem, in *IEEE Symposium on Computational Intelligence and Data Mining, 2007*. CIDM, 2007 (2007), pp. 535–539
46. R. Quick, V. Rayward-Smith, G. Smith, Fitness distance correlation and ridge functions, in *Parallel Problem Solving from Nature PPSN V*, vol. 1498, Lecture Notes in Computer Science, ed. by A. Eiben, T. Bäck, M. Schoenauer, H.P. Schwefel (Springer, Berlin Heidelberg, 1998), pp. 77–86
47. F. Rothlauf, *Representations for Genetic and Evolutionary Algorithms* (Springer, Secaucus, 2006)
48. J.R. Sherrah, R.E. Bogner, A. Bouzerdoum, The evolutionary pre-processor: automatic feature extraction for supervised classification using genetic programming, in *Proceedings of 2nd International Conference on Genetic Programming (GP-97)* (Morgan Kaufmann, Los Altos, 1997), pp. 304–312
49. S. Silva, J. Almeida, GPLAB—A Genetic Programming Toolbox for MATLAB, in *Proceedings of the Nordic MATLAB Conference* ed. by L. Gregersen, pp. 273–278 (2003)

50. S. Silva, E. Costa, Dynamic limits for bloat control in genetic programming and a review of past and current bloat theories. Genet. Program Evol. Mach. **10**(2), 141–179 (2009)
51. M. Smith, L. Bull, Genetic programming with a genetic algorithm for feature construction and selection. Genet. Program Evol. Mach. **6**(3), 265–281 (2005)
52. S.Y. Sohn, Meta analysis of classification algorithms for pattern recognition. IEEE Trans. Pattern Anal. Mach. Intell. **21**(11), 1137–1144 (1999)
53. A. Sotelo, E. Guijarro, L. Trujillo, L.N. Coria, Y. Martínez, Identification of epilepsy stages from ecog using genetic programming classifiers. Comput. Biol. Med. **43**(11), 1713–1723 (2013)
54. P. Stadler, Fitness landscapes, in *Biological Evolution and Statistical Physics*, vol. 585, Lecture Notes in Physics, ed. by M. Lässig, A. Valleriani (Springer, Berlin Heidelberg, 2002), pp. 183–204
55. T. Tanigawa, Q. Zhao, A study on efficient generation of decision trees using genetic programming, in *Proceedings of Genetic and Evolutionary Computation Conference (GECCO'2000), Las Vegas* (Morgan Kaufmann, Los Altos, 2000), pp. 1047–1052
56. M. Tomassini, L. Vanneschi, P. Collard, M. Clergue, A study of fitness distance correlation as a difficulty measure in genetic programming. Evol. Comput. **13**(2), 213–239 (2005)
57. L. Trujillo, Y. Martínez, E. Galván-López, P. Legrand, Predicting problem difficulty for genetic programming applied to data classification, in *Proceedings of the 13th Annual Conference on Genetic and Evolutionary Computation*, GECCO '11 (ACM, New York, 2011), pp. 1355–1362
58. L. Trujillo, Y. Martínez, E.G. López, P. Legrand, A comparative study of an evolvability indicator and a predictor of expected performance for genetic programming, in *Genetic and Evolutionary Computation Conference, GECCO '12, Philadelphia, PA, USA, July 7–11, 2012, Companion Material Proceedings* (2012), pp. 1489–1490
59. L. Trujillo, Y. Martínez, P. Melin, Estimating classifier performance with genetic programming, in *Proceedings of the 14th European conference on Genetic Programming*, EuroGP'11 (Springer, Berlin, 2011), pp. 274–285
60. L. Trujillo, Y. Martínez, P. Melin, How many neurons? A genetic programming answer, in *Proceedings of the 13th Annual Conference Companion on Genetic and Evolutionary Computation*, GECCO '11 (ACM, New York, 2011), pp. 175–176
61. A. Tsakonas, A comparison of classification accuracy of four genetic programming-evolved intelligent structures. Inf. Sci. **176**(6), 691–724 (2006)
62. L. Vanneschi, M. Castelli, L. Manzoni, The K landscapes: A tunably difficult benchmark for genetic programming, in *Proceedings of the 13th Annual Conference on Genetic and Evolutionary Computation*, GECCO '11 (ACM, New York, 2011), pp. 1467–1474
63. L. Vanneschi, M. Castelli, S. Silva, A survey of semantic methods in genetic programming. Genet. Program Evol. Mach. **15**(2), 195–214 (2014)
64. L. Vanneschi, M. Clergue, P. Collard, M. Tomassini, S. Verel, Fitness clouds and problem hardness in genetic programming, in *Proceedings of the Genetic and Evolutionary Computation Conference, GECCO'04*, pp. 690–701 (2004)
65. L. Vanneschi, M. Tomassini, P. Collard, M. Clergue, Fitness distance correlation in genetic programming: a constructive counterexample, in *Proceedings of the IEEE Congress on Evolutionary Computation*, CEC 2003, 8–12 December 2003, Canberra, Australia, pp. 289–296 (2003)
66. L. Vanneschi, M. Tomassini, P. Collard, S. Verel, Negative slope coefficient: a measure to characterize genetic programming fitness landscapes, in *Genetic Programming, 9th European Conference*, EuroGP 2006, Budapest, Hungary, April 10–12, 2006, Proceedings, pp. 178–189 (2006)
67. L. Vanneschi, M. Tomassini, P. Collard, S. Vérel, Y. Pirola, G. Mauri, A comprehensive view of fitness landscapes with neutrality and fitness clouds, in *Proceedings of the 10th European Conference on Genetic Programming*, EuroGP'07 (Springer, Berlin, Heidelberg, 2007), pp. 241–250
68. L. Vanneschi, A. Valsecchi, R. Poli, Limitations of the fitness-proportional negative slope coefficient as a difficulty measure, in *Proceedings of the 11th Annual Conference on Genetic and Evolutionary Computation*, GECCO '09 (ACM, New York, 2009), pp. 1877–1878
69. S. Verel, P. Collard, M. Clergue, Where are bottlenecks in NK fitness landscapes?, in *Proceedings of the IEEE Congress on Evolutionary Computation*, CEC 2003, 8–12 December 2003, Canberra, Australia, pp. 273–280 (2003)
70. D. Wolpert, W. Macready, No free lunch theorems for optimization. IEEE Trans. Evol. Comput. **1**(1), 67–82 (1997)
71. S. Wright, The roles of mutation, inbreeding, crossbreeding and selection in evolution. Proc. Sixth Int. Congr. Genet. **1**, 356–366 (1932)

72. T. Yu, J. Miller, Neutrality and the evolvability of boolean function landscape, in *Genetic Programming*, vol. 2038, Lecture Notes in Computer Science, ed. by J. Miller, M. Tomassini, P. Lanzi, C. Ryan, A. Tettamanzi, W. Langdon (Springer, Berlin, 2001), pp. 204–217
73. E. Z-Flores, L. Trujillo, O. Schütze, P. Legrand, A local search approach to genetic programming for binary classification, in *Proceedings of the 2015 on Genetic and Evolutionary Computation Conference*, GECCO '15 (ACM, New York, 2015), pp. 1151–1158
74. M. Zhang, W. Smart, Multiclass object classification using genetic programming, in *Applications of Evolutionary Computing*, vol. 3005, Lecture Notes in Computer Science, ed. by G. Raidl, S. Cagnoni, J. Branke, D. Corne, R. Drechsler, Y. Jin, C. Johnson, P. Machado, E. Marchiori, F. Rothlauf, G. Smith, G. Squillero (Springer, Berlin Heidelberg, 2004), pp. 369–378
75. M. Zhang, W. Smart, Using gaussian distribution to construct fitness functions in genetic programming for multiclass object classification. Pattern Recogn. Lett. **27**(11), 1266–1274 (2006)
76. Z.H. Zhou, *Ensemble Methods: Foundations and Algorithms*, 1st edn. (Chapman and Hall/CRC, London, 2012)